

Journal Pre-proof

H3K27me3 suppresses sister-lineage somatic gene expression in late embryonic germline cells of the ascidian, *Halocynthia roretzi*

Tao Zheng, Ayaki Nakamoto, Gaku Kumano



PII: S0012-1606(19)30499-3

DOI: <https://doi.org/10.1016/j.ydbio.2019.12.017>

Reference: YDBIO 8191

To appear in: *Developmental Biology*

Received Date: 20 August 2019

Revised Date: 21 November 2019

Accepted Date: 29 December 2019

Please cite this article as: Zheng, T., Nakamoto, A., Kumano, G., H3K27me3 suppresses sister-lineage somatic gene expression in late embryonic germline cells of the ascidian, *Halocynthia roretzi*, *Developmental Biology* (2020), doi: <https://doi.org/10.1016/j.ydbio.2019.12.017>.

This is a PDF file of an article that has undergone enhancements after acceptance, such as the addition of a cover page and metadata, and formatting for readability, but it is not yet the definitive version of record. This version will undergo additional copyediting, typesetting and review before it is published in its final form, but we are providing this version to give early visibility of the article. Please note that, during the production process, errors may be discovered which could affect the content, and all legal disclaimers that apply to the journal pertain.

© 2019 Published by Elsevier Inc.

1 H3K27me3 suppresses sister-lineage somatic gene expression in late embryonic
2 germline cells of the ascidian, *Halocynthia roretzi*

3 Tao Zheng, Ayaki Nakamoto and Gaku Kumano

4 Asamushi Research Center for Marine Biology, Graduate School of Life Sciences, Tohoku University

5

6 Corresponding author: Tao Zheng

7 Asamushi Research Center for Marine Biology

8 Graduate School of Life Sciences, Tohoku University

9 Asamushi Sakamoto 9, Aomori, Japan

10 +81-017-752-3390

11 zheng.tao.r2@dc.tohoku.ac.jp

12 Abstract

13 Protection of the germline from somatic differentiation programs is crucial for germ cell
14 development. In many animals, whose germline development relies on the maternally inherited germ
15 plasm, such protection in particular at early stages of embryogenesis is achieved by maternally
16 localized global transcriptional repressors, such as PIE-1 of *Caenorhabditis elegans*, Pgc of
17 *Drosophila melanogaster* and Pem of ascidians. However, zygotic gene expression starts in later
18 germline cells eventually and mechanisms by which somatic gene expression is selectively kept
19 under repression in the transcriptionally active cells are poorly understood.

20 By using the ascidian species *Halocynthia roretzi*, we found that H3K27me3, a repressive
21 transcription-related chromatin mark, became enriched in germline cells starting at the 64-cell stage
22 when Pem protein level and its contribution to transcriptional repression decrease. Interestingly,
23 inhibition of H3K27me3 together with Pem knockdown resulted in ectopic expression in germline
24 cells of muscle developmental genes *Muscle actin (MA4)* and *Snail*, and of *Clone 22* (which is
25 expressed in all somatic but not germline cells), but not of other tissue-specific genes such as the
26 notochord gene *Brachyury*, the nerve cord marker *ETR-1* and a heart precursor gene *Mesp*, at the
27 110-cell stage. Importantly, these ectopically expressed genes are normally expressed in the germline
28 sister cells (B7.5), the last somatic lineage separated from the germline. Also, the ectopic expression
29 of *MA4* was dependent on a maternally localized muscle determinant Macho-1. Taken together, we
30 propose that H3K27me3 may be responsible for selective transcriptional repression for somatic genes
31 in later germline cells in *Halocynthia* embryos and that the preferential repression of germline
32 sister-lineage genes may be related to the mechanism of germline segregation in ascidian embryos,
33 where the germline is segregated progressively by successive asymmetric cell divisions during cell
34 cleavage stages. Together with findings from *C. elegans* and *D. melanogaster*, our data for this
35 urochordate animal support the proposal for a mechanism, conserved widely throughout the animal
36 kingdom, where germline transcriptional repression is mediated initially by maternally localized
37 factors and subsequently by a chromatin-based mechanism.

39 **Keywords**

40 Ascidian; germline; H3K27me3; Pem; transcriptional repression; chromatin modification

41 1. Introduction

42 In some animals such as the insect *Drosophila*, the nematode *Caenorhabditis elegans*, ascidians, and
43 the amphibian *Xenopus*, segregation of the primordial germ cells (PGCs) from the somatic cell
44 lineage during early embryogenesis is tightly coupled with the inheritance of a distinct cytoplasm
45 known as the germ plasm, which contains essential factors for PGC development (Mahowald, 2001;
46 Ikenishi, 1998; Strome and Wood, 1982; Shirae-Kurabayashi et al., 2006; Heasman et al., 1984).
47 Examples of these maternally-localized factors include: PIE-1 of *C. elegans* (Batchelder et al.,
48 1999); Pgc of *Drosophila* (Hanyu-Nakamura et al., 2008); Nanos1 of *Xenopus* (Lai et al., 2012);
49 and Pem of the ascidians *Halocynthia roretzi* and *Ciona intestinalis* type A (currently called *Ciona*
50 *robusta*; Brunetti et al., 2015) (Kumano et al., 2011; Shirae-Kurabayashi et al., 2011). These factors
51 inhibit the phosphorylation of serine 2 in the carboxy-terminal domain (pSer2-CTD) of RNA
52 polymerase II (RNAPII) (Seydoux and Dunn, 1997; Batchelder et al., 1999; Hanyu-Nakamura et
53 al., 2008; Lai et al., 2012; Kumano et al., 2011; Shirae-Kurabayashi et al., 2011), a marker of
54 transcriptional elongation (Brookes and Pombo, 2009; Hsin and Manley, 2012), and thereby repress
55 gene expression globally in the early germline (Nakamura and Seydoux, 2008; Kumano, 2014;
56 Strome and Updike, 2015).

57 Transcriptional repression in germline development is pivotal for protecting the germline from
58 expressing somatic programs and thus for maintaining its totipotency to produce a new organism in
59 the next generation, which otherwise could lead to the apoptosis of germline cells or trans-fate into
60 somatic cells (Hayashi et al., 2004; Ciosk et al., 2006; Strome and Lehmann, 2007; Nakamura et al.,
61 2010; Strome and Updike, 2015; Pae et al., 2017; Gross-Thebing et al., 2017). Nevertheless, these
62 maternally localized factors responsible for transcriptional repression are only transiently present in
63 early germline cells. Furthermore, the strategy to prevent somatic programs in the germline by
64 global transcriptional repression might not be suitable at later stages of its development, because the
65 germline also needs to commence zygotic transcription in preparation for later germline-specific
66 events such as PGC migration, meiosis, and germ cell differentiation (Schäfer et al., 2003; Spencer

67 et al., 2011).

68 The mechanism underlying the selective transcriptional repression of somatic genes in later
69 germline cells is not well understood. Previous studies with *C. elegans* and *D. melanogaster* suggest
70 that transcriptional regulation in the germline switches from global transcriptional repression
71 mediated by maternally localized repressors (PIE-1 of *C. elegans* and Pgc of *Drosophila*) to
72 chromatin-dependent regulation when germline cells begin zygotic transcription (Strome and
73 Lehmann, 2007; Nakamura and Seydoux, 2008; Robert et al., 2015).

74 Ascidians, simple chordate animals in the Phylum Urochordata (Satoh et al., 2014), separate
75 germline cells progressively from somatic-fated cells during the cell cleavage stages of early
76 embryogenesis (Fig. 1). During the three successive unequal cell divisions from the 8-cell to the
77 64-cell stage (Fig. 1), germline cells (B4.1 at the 8-cell, B5.2 at the 16-cell, B6.3 at the 32-cell, and
78 B7.6 at the 64-cell stages) are one pair of the smallest cells remaining at the posterior end of the
79 embryo (Hibino et al., 1998; Nishikata et al., 1999; Shirae-Kurabayashi et al., 2006). In each of
80 these cleavages, the ascidian germ plasm (known as the centrosome-attracting body, CAB), is
81 inherited only by the germline cells (Hibino et al., 1998; Nishikata et al., 1999; Shirae-Kurabayashi
82 et al., 2006). Molecular studies of CAB components have revealed that a number of maternal
83 mRNAs called *Postplasmic/PEM* RNAs are enriched in CAB (Yoshida et al., 1996; Prodon et al.,
84 2007; Makabe and Nishida, 2012). These mRNA factors associated with CAB are essential for
85 germline development, such as *Popk-1* for CAB formation (Sasakura et al., 2000; Nakamura et al.,
86 2005; Miyaoku et al., 2018) and *Pem* and *Zf-1* for germline transcriptional regulation (Yoshida et
87 al., 1996; Sasakura et al., 2000; Kumano et al., 2011; Shirae-Kurabayashi et al., 2011; Miyaoku et
88 al., 2018), as well as other kinds of embryonic regulation (Yoshida et al., 1996; Nishida and
89 Sawada, 2001; Kobayashi et al., 2003; Kumano and Nishida, 2009). In addition, the localization of
90 a conserved germline marker (Vasa mRNA and protein) to CAB has been observed
91 (Shirae-Kurabayashi et al., 2006).

92 In ascidians, zygotic gene expression starts at the 4- (*H. roretzi*) or 8-cell (*C. intestinalis*) stages
93 in somatic cells (Kumano et al., 2011; Treen et al., 2018), whereas in *H. roretzi* it has been
94 suggested that zygotic germline gene expression initiates between the 110-cell stage and the early
95 gastrula (Miyaoku et al., 2018). Only a weak phosphorylation of serine 5 of the carboxy-terminal
96 domain of RNAPII (pSer5-CTD), a marker of transcriptional initiation (Brookes and Pombo, 2009;
97 Hsin and Manley, 2012), and almost no pSer2-CTD are detected in germline cells at the 8- and
98 16-cell stages in *H. roretzi* (Kumano et al., 2011). In *C. intestinalis* type A, however, weaker pSer5-
99 and pSer2-CTD signals are observed in germline cells at the 8-, 16-, 32-, and 110-cell stages when
100 compared to somatic cells (Shirae-Kurabayashi et al., 2011). The transcriptional quiescence in early
101 germline cells at the 8- and 16-cell stages in these two species has been shown to be mediated by a
102 maternally localized factor, Pem (as described above), whose mRNA and protein are enriched in
103 CAB and its protein in germline nuclei (Kumano et al., 2011; Shirae-Kurabayashi et al., 2011). In
104 contrast to *C. intestinalis* type A, however, pSer2-CTD in *H. roretzi* has been detected in germline
105 cells at the 32-, 64- and 118-cell stages at a comparable level to that in somatic cells (Tomioka et al.,
106 2002). Consistent with this, while all the somatic genes tested showed ectopic expression in
107 germline cells upon Pem knockdown at the 16-cell stage, only a subset of genes did so at the 32-cell
108 stage (Kumano et al., 2011). In addition, anti-Pem antibody staining shows that the Pem protein
109 level decreases as development proceeds and the decrease starts during the 32- and 64-cell stages
110 (Negishi et al., 2007). These results suggest that the contribution of Pem to transcriptional
111 repression in the germline declines starting at the 32-cell stage in *H. roretzi* embryos. A recent study
112 unveiled the function of another maternally localized factor to CAB: Zf-1 is an RNA binding
113 protein responsible for down-regulating Pem protein level, thereby allowing zygotic germline gene
114 expression between the 110-cell stage and early gastrula (Miyaoku et al., 2018).

115 All these observations in *H. roretzi* suggest that Pem alone may no longer protect the germline
116 from expressing somatic genes around the time when zygotic germline gene expression
117 commences. However, in general, the somatic transcripts are still faithfully repressed in the

118 germline (Strome and Lehmann, 2007; Strome and Updike, 2015), so it is of interest to determine
 119 how the later germline cells distinguish the regulation of desired germline-specific genes from
 120 unfavorable somatic programs. To investigate this (using *H. roretzi*), it is of particular interest to
 121 discover (1) whether or not Pem protein still represses somatic gene expression in later germline cells,
 122 and (2) if there are any other factors that repress the transcription of somatic genes following the
 123 decrease of Pem protein levels.

124 Here, we first confirmed that Pem is still required for downregulating the activity of RNAPII in
 125 germline cells at the 110-cell stage. In addition, we found that a repressive transcription-related
 126 chromatin modification, H3K27me3, becomes evident in germline cells from the 64-cell stage
 127 onwards and that both H3K27me3 and Pem are required to repress somatic gene expression in the
 128 germline cells at the 110-cell stage. Finally, we found that somatic genes ectopically expressed in
 129 110-cell stage germline cells upon the inhibition of H3K27me3 and Pem are those normally
 130 expressed in the B7.5 lineage, the last lineage that is separated from the germline (Fig. 1).
 131 Collectively, our current study suggests that H3K27me3 may be a selective factor to keep somatic
 132 gene expression suppressed in *Halocynthia* germline cells even after the global transcriptional
 133 repression has been lifted and zygotic gene expression has started. It is proposed that
 134 chromatin-based mechanisms following those of maternally localized factors for transcriptional
 135 repression regulation in the germline may be conserved across animal species.

136

137 2. Material and Methods

138 2.1. Animals and embryos

139 Adult *H. roretzi* were purchased from local fishermen or collected in the sea near the Asamushi
140 Research Center for Marine Biology before their natural spawning season starts in early winter. To
141 restrain *H. roretzi* from spawning before use in the laboratory, the animals were kept in tanks under
142 constant light at 8°C. Spawning was induced by light stimuli after leaving the animals in darkness
143 for more than 6 hours and by warming the seawater to 11-13°C. Eggs were fertilized with
144 non-self-sperm. Embryos were cultured in Millipore-filtered seawater (MFSW) containing 50 mg/L
145 streptomycin sulfate (Sigma) and 50 mg/L kanamycin sulfate (Wako) at 9-13°C.

146

147 2.2. Microinjection, GSK126 inhibitor and Cytochalasin B treatment

148 Specific morpholino antisense oligonucleotide (MO, Gene Tools) against *Pem*
149 (Harore.CG.MTP2014.S480.g14149 in Aniseed database: <https://www.aniseed.cnrs.fr/aniseed/>) was
150 prepared as described previously (Kumano et al., 2011). As a control, the standard MO (NC MO)
151 provided by Gene Tools was used. En^R-Macho-1 mRNA was prepared to suppress the function of
152 Macho-1 (Zic-r.a, Harore.CG.MTP2014.S236.g13376) as described previously (Kumano et al.,
153 2010). Microinjection of MO or mRNA was performed according to the method of Kumano (2018).
154 Approximately 180 to 250 pg of Pem or NC MO was injected depending on how far we were into
155 the spawning season. For mRNA injection, approximately 25 pg of Macho-1-En^R mRNA was
156 injected.

157 To inhibit H3K27me3, a selective inhibitor of EZH2 methyltransferase, GSK126, (McCabe et
158 al., 2012; Kaniskan et al., 2018) was purchased (Cayman Chemical) and kept at -30°C in DMSO at
159 14.7 mM (stock). Prior to use, the stock solution was diluted in MFSW to a concentration of 50 μM.
160 As a control, the same volume of DMSO was added to MFSW. Approximately half of the injected
161 or un-injected eggs were randomly transferred into MFSW containing either 50 μM GSK126 or
162 DMSO.

163 Cytochalasin B (Wako) treatment to arrest cell divisions was performed as reported previously
164 (Kobayashi et al., 2003).

165

166 2.3. Immunostaining

167 Immunostaining for *H. roretzi* embryos was performed as described by Kumano et al. (2011),
168 with the following modifications. (1) Embryos were fixed overnight (over 16 hours) at 4°C with 4%
169 paraformaldehyde in fixation buffer (0.5 M NaCl, 0.1 M MOPS, pH 7.5) for all the antibodies used
170 in this study. (2) Primary antibodies were used at the following concentrations: H5 antibody against
171 pSer2-CTD of RNAPII (covance, MMS-129R) and antibodies against H3K27me3 (abcam,
172 EPR18607), H3K4me3 (abcam, ab8580) and DNA methylation (abcam, ab73938) at 1: 5000; and
173 antibodies against H3K4me2 (abcam, ab32356), H3K9me3 (abcam, EPR16601) and H3K9me2
174 (abcam, ab32521) at 1:1,000.

175

176 2.4. SYTOX nuclear staining

177 Nuclei were stained with SYTOX green (Invitrogen) after immunostaining and whole-mount *in*
178 *situ* hybridization. The SYTOX green stock was prepared at 5 mM in DMSO and kept at -30°C.
179 Prior to use, the stock solution was diluted in 0.05 M Tris-HCl pH 7.4 containing 0.15 M NaCl.
180 Stained samples after immunostaining and whole-mount *in situ* hybridization were washed in
181 Solution A (0.5 M NaCl, 5 mM EDTA, 10 mM Tris 0.1% Tween 20, pH 8.0) for 5 minutes.
182 Additionally, the samples after immunostaining were then treated with 100 µg/mL of RNase A in
183 solution A for 1 hour at 37°C. After washing in 0.05 M Tris-HCl pH 7.4 containing 0.15 M NaCl (3
184 times, 5 minutes each), samples were incubated with 2 µM SYTOX green solution and then washed
185 3 times (5 minutes each) with 0.05 M Tris-HCl pH 7.4 containing 0.15 M NaCl for observation.

186

187 2.5. Mounting and quantification of fluorescent signal intensity

188 Specimens were mounted in 80% glycerol in PBS and observed with a confocal microscope
189 LSM5 PASCAL (ZEISS). To quantify the pSer2-CTD, H3K27me3 and SYTOX green signals in
190 nuclei, Z stack images were created by the average-intensity method using each of the Z section
191 images containing the fluorescent nuclear signals. The areas of the nuclei were then selected using
192 the polygon selection tool in ImageJ and the fluorescent intensities in the areas were quantified with
193 the measurement tool in ImageJ. All the images compared were obtained under the same conditions.
194 The relative H3K27me3 or pSer2-CTD signals were calculated by dividing the signal intensity
195 (quantified values) of H3K27me3 or pSer2-CTD, respectively, by that of SYTOX green observed in
196 the same nuclei. The relative intensities were statistically compared using the Mann-Whitney U test.

197

198 2.6. Whole-mount *in situ* hybridization

199 Whole-mount *in situ* hybridization for *H. roretzi* embryos was performed using
200 digoxigenin-labeled probes as described by Wada et al. (1995). To make antisense probes for *Tbx6*
201 (Harore.CG.MTP2014.S461.g12970) and *Mesp* (Harore.CG.MTP2014.S97.g06901), fragments
202 were PCR-amplified with the specific primers described below, using as templates the plasmid *Tbx6*
203 in PBS-HTB(N) (Kumano et al., 2014) for *Tbx6* and a cDNA library generated from extracted
204 mRNA from early gastrula embryos with SMARTer™ RACE cDNA Amplification Kit (Clontech)
205 for *Mesp*.

206 To make antisense probes for *Mhc-1* (Harore.CG.MTP2014.S198.g07633), *Ezh*
207 (Harore.CG.MTP2014.S59.g15552), *Eed* (Harore.CG.MTP2014.S326.g09247), *Suz12*
208 (Harore.CG.MTP2014.S68.g10825), *Rbbp4/7-r.a* (Harore.CG.MTP2014.S14.g04532) and
209 *Rbbp4/7-r.b* (Harore.CG.MTP2014.S12.g03265), fragments were obtained with Rapid amplification
210 of cDNA ends (RACE) experiments (3' RACE for *Mhc-1* and 5' RACE for other genes), in which a
211 cDNA library generated from extracted mRNA from early gastrula embryos with SMARTer™

212 RACE cDNA Amplification Kit was used as the template and the gene-specific primers (GSP) and
213 nested gene-specific primers (nGSPs) listed below were used in combination with the primers
214 offered in the SMARTer™ RACE cDNA Amplification Kit. All the PCR products were sub-cloned
215 into the pGEM-T Easy vector (Promega), and the sub-cloned plasmids were then digested with
216 appropriate restriction enzymes to linearize and served as templates for *in vitro* transcription using
217 T7 or SP6 RNA polymerase (Roche). As a negative control for *in situ* hybridization for the PRC2
218 components, a sense probe for *Ezh* was used.

219 Primer sets used for cloning the genes were as follows:

220 *Tbx6*: (Forward) 5'-GGTCGAAGTGGATGAGCGA-3'

221 and (Reverse) 5'-GTGATGCCGTTCTGGGTGTA-3'

222 *Mesp*: (Forward) 5'-TTATCAGATTACCAGTATAG -3'

223 and (Reverse) 5'-TAAATTACCACAATATGAATC-3'

224 and (Nested PCR Forward) 5'-GGAACAGACAAGTACATCCA-3'

225 *Mhc-1*: (GSP) 5'-ACTTGGGCATGCAACACGACAAGCTTCTGA-3'

226 and (nGSP) 5'-CCGCTCTTGAACAAGCGGAACGAGGAAGA-3'

227 *Ezh*: (GSP) 5'-CTCCACAGGCTTCATTACCAGGCTT-3'

228 and (nGSP) 5'-GCTCTCTCTGCACCGACTTGCATTA-3'

229 *Eed*: (GSP) 5'-GCCATATTGGTTCCGAGAGCCAGA-3'

230 and (nGSP) 5'-AGCCAGGTTCCAACAGACCAAGTG-3'

231 *Suz12*: (GSP) 5'-CCCGGCTGGCTGAAAATGTTTGCAGGA-3'

232 and (nGSP) 5'-CTCTGCCCATCGAACGATTCCCACA-3'

233 *Rbbp4/7-r.a*: (GSP) 5'-GCAGTTAACCTCGGCTGTGTGCCT-3'

234 and (nGSP) 5'-TGGTCGTCAGCCACCGATCCGAACAA-3'

235 *Rbbp4/7-r.b:* (GSP) 5'-CGGTTTATCCGAGGACCCGGTAGCGA-3'

236 and (nGSP) 5'-CGTGGGCTACGATCGCGTGAATAGGT-3'

237

238 For *in situ* hybridization of *Muscle actin (MA4)* (Harore.CG.MTP2014.S575.g07280)

239 (Kusakabe et al., 1991), *Clone 22* (Tomioka et al., 2002), *Brachyury*

240 (Harore.CG.MTP2014.S42.g07916) (Yasuo and Satoh, 1998), *ETR-1*

241 (Harore.CG.MTP2014.S5.g02306) (Yagi and Makabe, 2001) and *ADP/ATP translocase*

242 (Harore.CG.MTP2014.S737.g07016) (Miya et al., 1994), the plasmid containing each of these

243 clones was kindly provided by Dr. Hiroki Nishida (Osaka University) and used as a template to

244 make antisense probes by *in vitro* transcription. The specimens were mounted and observed with a

245 microscope (BX51, Olympus).

246

247 2.7. Phylogenetic analyses

248 Molecular phylogenetic analyses were carried out with full-length amino acid sequences of

249 *Mesp*, and the core PRC2 components. The putative sequences of *Mesp* and PRC2 components were

250 obtained by BLAST search in the ascidian genome database Aniseed using a *Ciona* sequence for

251 *Mesp* and mammalian sequences for the PRC2 components as queries.

252 Sequence alignments were conducted using the MUSCLE algorithm offered in the Molecular

253 Evolutionary Genetics Analysis software (MEGA7; Kumar et al., 2016). Gaps in the amino-acid

254 alignments were manually deleted. Phylogenetic trees were constructed using the

255 neighboring-joining method in the MEGA7. Bootstrap replications (1000 replications) were

256 conducted to estimate tree reliability.

257

258 3. Results

259 3.1. Pem represses pSer2-CTD of RNAPII in the germline at a later stage

260 Previous work showed that Pem represses somatic gene expression in early germline
 261 blastomeres (B3 at the 4-cell stage, B4.1 at the 8-cell stage, B5.2 at the 16-cell stage; Fig. 1) by
 262 inhibiting pSer2-CTD of RNAPII and transcriptional elongation in *H. roretzi* (Kumano et al., 2011).
 263 However, several past observations imply that the contribution of Pem to transcriptional repression
 264 in germline cells may decrease from the 32-cell stage onwards (Tomioka et al., 2002; Negishi et al.,
 265 2007; Kumano et al., 2011; Miyaoku et al., 2018), as mentioned above. Thus, we were curious to
 266 investigate whether or not Pem still represses pSer2-CTD of RNAPII after the 32-cell stage.

267 As a first step to investigate this, we re-examined the level of pSer2-CTD of RNAPII at the 16-
 268 and 110-cell stages using a different antibody staining method from that used by Tomioka et al.
 269 (2002), who demonstrated that the levels of positive pSer2-CTD signals are comparable to somatic
 270 cells in the germline at the 32-, 64- and 118-cell stages. We fixed embryos in 4% paraformaldehyde
 271 (not in -20°C methanol as described in Tomioka et al., 2002), and detected HRP activity on the
 272 secondary antibody using the TSA Plus Cy3 kit (Perkin-Elmer Life Science); this was without the
 273 combination of Biotinyl-Tyramide (TSA kit, NEN Life Science Products) and Alexa streptavidin
 274 (Molecular Probes) as described by Tomioka et al. (2002). As previously reported (Kumano et al.,
 275 2011), we confirmed that pSer2-CTD is detectable in somatic cells (yellow arrows in Fig. 2B) but
 276 not in germline cells at the 16-cell stage (0%, n = 13; white arrows in Fig. 2B, B'). In contrast,
 277 110-cell stage germline cells displayed a recognizable although weak pSer2-CTD signal (when
 278 compared to that in somatic cells: 50%, n = 14; red arrows in Fig. 2D, D'). This is consistent with
 279 the previous report with anti-Pem antibody staining showing that the amount of Pem protein is
 280 decreased as development proceeds (Negishi et al., 2007). We also noticed that the detection of
 281 positive pSer2-CTD signal seems to be affected by the cell cycle, as we have not seen positive
 282 signals in anaphase nuclei (purple arrows in Fig. 2C, D) whereas the same blastomere not
 283 undergoing cell division in a different embryo showed positive pSer2-CTD (green arrows in Fig.
 284 2E, E'). Considering that germline cells at the 110-cell stage do not undergo cell division at least

285 until gastrulation (Nishida, 1986; Shirae-Kurabayashi et al., 2006), the absence of or lower
 286 pSer2-CTD observed in the germline cells may indicate that pSer2-CTD at this stage is still under
 287 repression.

288 To test this hypothesis, we tried to knock down Pem by injecting fertilized eggs with a
 289 morpholino antisense oligonucleotide (MO) against Pem and examined whether pSer2-CTD of
 290 RNAPII in the germline would be enhanced. Ectopic germline pSer2-CTD was observed in the
 291 16-cell stage germline cells when injected with Pem MO (61.5%, n = 13; red arrow in Fig. S1) as
 292 previously reported (Kumano et al., 2011), validating the Pem knockdown effect in our experiment.
 293 Next, we examined pSer2-CTD levels in germline cells of Pem morphant at the 110-cell stage and
 294 found that stronger signals for pSer2-CTD were detected in the cells than those in the un-injected or
 295 negative control (NC) MO-injected embryos (red arrows in Fig. 2E'', F'', G''). This increased
 296 germline signal for pSer2-CTD after Pem knockdown was confirmed by quantifying the signal
 297 intensity ($p < 0.001$, Mann-Whitney U test in Fig. 2H). Thus, these results suggest that Pem continues
 298 to repress the activity of RNAPII through the later embryonic stage when zygotic germline gene
 299 expression starts (Miyaoku et al., 2018).

300

301 3.2. H3K27me3 is enriched in later embryonic germline cells

302 To examine whether other factors might be involved in germline transcriptional regulation at
 303 later stages, we conducted immunostaining with antibodies against DNA methylation and histone
 304 modifications (Fig. S2; Table S1) including heterochromatin marks H3K9me2 and H3K9me3, active
 305 chromatin modifications H3K4me2 and H3K4me3 and a repressive transcription mark H3K27me3.
 306 We specifically examined whether any marks would show different patterns between germline and
 307 somatic cells and between the early and later stages.

308 Table S1 summarizes our immunostaining results, showing that DNA methylation and
 309 H3K9me2 were almost undetectable in both germline and somatic cells at all stages tested (from the

310 16-cell to 110-cell stages), while H3K9me3 and H3K4me2/3 did not show any significant
 311 differences in signal intensity between germline and somatic cells as well as between early and late
 312 stages (Fig. S2; Table S1). However, in light of our observation on H3K27me3, as described below,
 313 we decided to further test the possible involvement of H3K27me3 in transcriptional regulation in
 314 the later stage of *H. roretzi* germline cells.

315 We found that the intensity of H3K27me3 signal markedly increased in the germline from the
 316 64-cell stage onwards (red arrows in Fig. 3Ad, d', e, e', f, f'), although its level in somatic cells of
 317 the vegetal region also increased (Fig. 3Ad, d', e, e', f, f'). These observations were confirmed by
 318 assessing the average intensities of fluorescent nuclear signals from confocal Z-stack images (Fig.
 319 3B). The quantitative analyses also showed that the germline cells exhibited the highest level of
 320 H3K27me3 among all the blastomeres at the 110-cell stage (Fig. 3C). Germline sister cells B7.5 and
 321 nerve cord cells, which appeared to show the strongest signal among the somatic cells, were chosen
 322 for the comparison with germline cells (Fig. 3C). Given that H3K27me3 is a mark related to
 323 repressive transcription, its enrichment in these later embryonic germline cells implies its potential
 324 role in repressing transcription in the cells.

325
 326 3.3. The core PRC2 components in *H. roretzi* are maternally supplied

327 H3K27me3 is catalyzed by a conserved complex called PRC2 (Lee et al., 2006; Simon and
 328 Kingston, 2009; Prokopuk et al., 2017), which in human cells comprises four core components:
 329 EZH1/2, SUZ12, EED, RBBP4/7 (Margueron and Reinberg, 2011). In an attempt to understand the
 330 mechanism of the enrichment of H3K27me3 in the later ascidian embryonic germline cells, we
 331 decided to clone these core components from *H. roretzi*. Using the human sequences as queries, we
 332 used BLAST to search for *H. roretzi* orthologs of core PRC2 components in the *H. roretzi* genome.
 333 We obtained single orthologous genes of EZH1/2, SUZ12 and EED as the best hits (which refer to
 334 as *Ezh*, *Suz12* and *Eed*, respectively), and two orthologous genes of RBBP4/7, namely *Rbbp4/7-r.a*
 335 and *Rbbp4/7-r.b*. These genes were confirmed as *H. roretzi* orthologues by phylogenetic analyses

336 (Fig. S3).

337 We then carried out whole-mount *in situ* hybridization for each of the PRC2 components (Fig.
338 S4), and found that all the components showed a similar expression pattern that they were expressed
339 at a high level in eggs, suggesting that they are maternally supplied, had more transcripts in the
340 animal than vegetal hemispheres from the 8-cell to the 110-cell stage (Fig. S4), and showed no
341 enrichment of mRNAs in germline cells at later stages (at the 64- and 110-cell stages; black arrows
342 in Fig. S4) when increased levels of H3K27me3 were observed. Thus, we were unable to discover
343 how H3K27me3 becomes enriched in germline cells from the 64-cell stage onwards from the *in situ*
344 hybridization results. Further clarification is to be expected from future studies of protein
345 localization.

346

347 3.4. Pem- and H3K27me3-deficient germline shifts towards sister cell muscle fate

348 Data presented thus far show that Pem still represses the activity of RNAPII in 110-cell stage
349 germline cells and that H3K27me3 may be involved in regulating germline transcription. We
350 therefore asked whether Pem or H3K27me3 or both are required to repress somatic gene expression
351 in later embryonic germline cells. To investigate this, we decided to test the occurrence of ectopic
352 somatic gene expression in the germline where the levels of Pem or H3K27me3 or both are
353 reduced. To inhibit H3K27me3, we used inhibitor GSK126. After testing different concentrations,
354 we confirmed that embryos treated with 50 µM GSK126 developed and hatched normally (100%, n
355 = 20), but displayed a great reduction in H3K27me3 levels (white arrows in Fig. 4A).

356 We found that two muscle developmental genes, *Muscle actin (MA4)* and *Snail*, among other
357 tissue-specific genes tested, were ectopically expressed in germline cells (Figs. 4 and 5). In normal
358 110-cell stage embryos, the *MA4* gene is expressed specifically in a pair of five muscle cells (Fig.
359 4Ba) (Kusakabe et al., 1991; Kusakabe, 1995). We did not detect mis-expression of *MA4* in B7.6
360 germline cells at the 110-cell stage after GSK126 treatment (Figs. 4Bb, C and S5), suggesting that

361 the depletion of H3K27me3 alone is not enough to de-repress *MA4* gene expression in the 110-cell
 362 stage germline. Similarly, embryos that had been treated with the inhibitor and injected with 250 pg
 363 of NC MO did not exhibit ectopic *MA4* gene expression in the germline (Figs. 4Bc, C and S5),
 364 indicating that MO injection itself would not cause ectopic *MA4* expression. In contrast, ectopic
 365 *MA4* expression in germline cells was observed after Pem MO injection (Figs. 4Bd, C and S5).
 366 Notably, significantly more embryos showed ectopic *MA4* expression in the germline when Pem
 367 and H3K27me3 were simultaneously depleted than when Pem alone was knocked down (Figs. 4Be,
 368 C and S5). These results indicate that H3K27me3 contributes to preventing *MA4* from being
 369 expressed in the germline at the 110-cell stage, although this effect could only be seen in the Pem
 370 knockdown background.

371 Intriguingly, *MA4* was not the only muscle developmental gene that showed ectopic expression
 372 in the germline. Our *in situ* hybridization results discovered the ectopic expression of *Snail* (Wada
 373 and Saiga, 1999; Sawada et al., 2005) (Fig. 4Bf-j). Expression of the *Snail* gene is not restricted to
 374 muscle cell lineages but also occurs in precursor cells of mesenchyme, notochord and neural tube
 375 (Wada and Saiga, 1999). However, previous studies have shown that this gene is important for
 376 muscle development in *Ciona* embryos (Fujiwara et al., 1998; Tokuoka et al., 2018). Similar to the
 377 results for *MA4* expression, we found that ectopic *Snail* expression was observed in Pem- and
 378 H3K27me3-deficient germline cells at the 110-cell stage (Figs. 4Bj, D and S6), but not in germline
 379 cells treated with DMSO (Figs. 4Bf, D and S6), the inhibitor alone (Figs. 4Bg, D and S6) or the
 380 inhibitor + NC MO (Figs. 4Bh, D and S6). For *Snail*, in contrast to *MA4*, Pem knockdown alone did
 381 not cause ectopic expression (Figs. 4Bi, D and S6). Taken together, these data support the
 382 hypothesis that Pem and H3K27me3 protect germline cells from expressing muscle developmental
 383 genes.

384 During the above analyses, injection of Pem MO sometimes caused abnormal cleavage
 385 patterns, especially in the posterior region of the embryo, probably because Pem is bifunctional,
 386 regulating also cell division patterns in ascidians (Negishi et al., 2007). It also sometimes resulted in

387 the loss of endogenous *MA4* expression (light blue arrows in Fig. S7C, E; Fig. S7D) similar to a
 388 previous report for the loss of Myosin expression upon Pem knockdown (Kumano and Nishida,
 389 2009). These effects made it difficult to recognize germline cells; therefore, we always stained
 390 nuclei to recognize each cell and managed to identify the cells by their smallest cell size, a
 391 characteristic of the germline cells (see Fig. S7 for further details).

392 In an effort to search for genes showing ectopic expression in the germline, we did not detect
 393 the ectopic expression of tissue-specific genes other than muscle, namely heart, nerve cord, and
 394 notochord developmental genes. We first searched for the heart marker gene *Mesp* in the *H. roretzi*
 395 genome database (Aniseed <https://www.aniseed.cnrs.fr>), identifying a gene with the best hit in a
 396 BLAST search against the database, using *Ciona Mesp* as a query (Satou et al., 2004), and
 397 confirmed by phylogenetic analysis that it is the *Halocynthia* orthologue of *Mesp* (Fig. S8). *In situ*
 398 hybridization showed that it was exclusively expressed in the heart precursor cells (B7.5 cell) at the
 399 110-cell stage (Fig. 5Ab). With this gene as a marker for heart differentiation, we found that Pem-
 400 and H3K27me3-deficient embryos showed no ectopic *Mesp* expression in germline cells (0%, n =
 401 13; yellow arrows in Fig. 5Ab') whereas other embryos with the same treatment and from the same
 402 batch showed ectopic *Snail* expression serving as a positive control (20%, n = 15; red arrow in Fig.
 403 5Aa'). For a notochord developmental gene, we studied notochord-specific *Brachyury* gene
 404 expression (Yasuo and Satoh, 1998) and found that embryos lacking Pem and H3K27me3
 405 ectopically expressed this gene in B7.5 and other posterior vegetal cells, but not in germline cells
 406 (0%, n = 8; yellow arrows in Fig. 5Bb'). Embryos from the same batch showed ectopic *MA4*
 407 expression in the germline (75%, n = 8; red arrow in Fig. 5Ba'). We note that we sometimes
 408 observed *Brachyury* expression in B8.5 mesenchyme cells, sister cells to notochord B8.6 (gray
 409 arrows in Fig. 5Bb). Also, previous studies have shown that after Pem knockdown ectopic
 410 *Brachyury* expression appears in posterior vegetal blastomeres (Kumano and Nishida, 2009).
 411 Finally, for a nerve cord developmental gene, we used *ETR-1* (Yagi and Makabe, 2001), and no
 412 ectopic *ETR-1* expression in the germline was observed in Pem- and H3K27me3-deficient germline

413 cells (0%, n = 19; yellow arrows in Fig. 5Cb'). Embryos from the same batches showed ectopic
 414 expression of *Clone 22* (see below), serving as a positive control (56.3%, n = 16; red arrows in Fig.
 415 5Ca').

416 Thus, the current study suggests that Pem- and H3K27me3-deficient germline cells tend to
 417 express muscle developmental genes rather than other somatic genes. Interestingly, muscle (and
 418 heart) is the last somatic lineage that is separated from the germline (Fig. 5D). Therefore, germline
 419 cells may take on the fate of their sister lineage in ascidian embryos when transcriptional regulation is
 420 compromised.

421

422 3.5. Pem- and H3K27me3-deficient germline cells do not become fully differentiated as muscle nor
 423 express a later germline marker

424 We next examined whether Pem- and H3K27me3-deficient germline cells become fully
 425 differentiated muscle cells. To investigate this, we studied the expression of other muscle
 426 developmental genes: *Myosin heavy chain* (*Mhc-1*; Makabe and Satoh, 1989; Makabe et al., 1990),
 427 a muscle structural gene; and *Tbx6* (Mitani et al., 1999), encoding a T-box transcription factor
 428 essential for muscle development (Mitani et al., 1999, 2001; Yagi et al., 2004; Sawada et al., 2005).
 429 At the 110-cell stage, ectopic *Mhc-1* and *Tbx6* expression was not observed in germlines deficient
 430 in Pem- and H3K27me3 (0%, n = 58 for *Mhc-1* in Fig. 6Ab'; 1.96%, n = 51 for *Tbx6* in Fig. 6Bb'),
 431 while mis-expression of *MA4* was readily observed in embryos from the same batches (12.9%, n =
 432 62, for positive control for *Mhc-1* in Fig. 6Aa'; 9.68%, n = 62 for *Tbx6* in Fig. 6Ba'). Thus, these
 433 results reveal that not all the muscle developmental genes were mis-expressed after decreasing the
 434 levels of Pem and H3K27me3, suggesting that Pem- and H3K27me3-deficient germline cells only
 435 partially take on a muscle differentiation profile.

436 We then examined whether or not germline cells with ectopic somatic gene expression still
 437 retain germline features. For this, we investigated the expression of a germline marker *ADP/ATP*

438 *translocase* (Miya et al., 1994; Miyaoku et al., 2018) at the tailbud stage. We found that embryos
 439 developed no *ADP/ATP translocase* expression in germline cells located at the tip of the tail when
 440 either Pem was knocked down (56.3%, n = 16; light blue bar without red arrows in Fig. 6Cb) or both
 441 Pem and H3K27me3 levels were downregulated (44%, n = 25; light blue bar without red arrows in
 442 Fig. 6Cc). Although there was no significant difference in percentage of embryos having no
 443 *ADP/ATP translocase* expression in the germline between these two treatments, the percentages
 444 themselves were much higher than those of embryos with ectopic somatic gene expression (e.g.
 445 13.9% for *MA4* and 11.2% for *Snail* when Pem and H3K27me3 were downregulated, Fig. 4);
 446 therefore, the *ADP/ATP translocase* expression was likely eliminated at the tailbud stage mainly by
 447 unknown mechanisms as a result of Pem knockdown possibly acting after the 110-cell stage.
 448 Therefore, we were not able to determine whether the mis-regulation of germline transcription at the
 449 110-cell stage prevents germline cell from retaining germline features at the tailbud stage.

450

451 3.6. Ectopic *MA4* expression depends on a maternal muscle determinant, Macho-1

452 We next asked why *Halocynthia* germline cells favored the expression of muscle
 453 developmental genes when somatic gene expression was no longer suppressed. Muscle fate in
 454 ascidian embryos is specified by two different mechanisms. Muscle cells located at the posterior tip
 455 of the tadpole larval tail are derived from the anterior-vegetal lineage (A4.1 lineage); are formed by
 456 inductive signals from neighboring cells (Meedel et al., 1987; Tokuoka et al., 2007); and are
 457 classified as secondary muscle cells. In contrast, muscle cells in the anterior and majority part of the
 458 tadpole larval tail are derived from the posterior-vegetal lineage (B4.1 lineage, Fig. 5D); are
 459 specified cell-autonomously by inheritance of a maternally localized muscle determinant, Macho-1
 460 (Nishida and Sawada, 2001; Satou et al., 2002; Sawada et al., 2005); and are classified as primary
 461 muscle cells. However, Macho-1 is unnecessary for secondary muscle formation (Nishida and
 462 Sawada, 2001; Sawada et al., 2005). Interestingly, a primary muscle lineage, the B7.5 lineage,
 463 which contains also heart fate, is the last somatic lineage separated from the germline during cell

464 cleavages (Fig. 5D). Therefore, the germline could easily contain Macho-1 as it is the sister lineage
 465 to B7.5. In fact, maternal *Macho-1* mRNA is localized to CAB and inherited by the germline
 466 (Nishida and Sawada, 2001; Satou et al., 2002). This raises the possibility that the ectopic muscle
 467 program in the germline may be due to the presence of Macho-1. To test this possibility, we studied
 468 whether inhibition of Macho-1 activity in Pem- and H3K27me3-deficient embryos would prevent
 469 ectopic *MA4* expression. To inhibit the function of Macho-1, we took advantage of a
 470 dominant-negative form of Macho-1 (Sawada et al., 2005; Kumano et al., 2010), referred to as
 471 En^R-Macho-1, in which the full-length Macho-1 is fused with the *Drosophila* Engrailed
 472 transcriptional repressor domain (Sawada et al., 2005; Kumano et al., 2010). We found that
 473 inhibition of Macho-1 function eliminated ectopic *MA4* expression caused by downregulation of
 474 Pem and H3K27me3 (33%, n = 12; Fig. 7B, D) in almost all cases (4.8% expression, n = 21; Fig.
 475 7C, D) as well as endogenous expression (Fig. 7C), indicating that the ectopic expression depends
 476 on Macho-1. This result also highlights the importance of Pem and H3K27me3 in restricting the
 477 function of transcription factors effective outside the germline.

478

479 3.7. Pem- and H3K27me3-deficient germline also mis-expresses a ubiquitous gene

480 We next used *Clone 22* as an example of a somatic gene expressed in all the blastomeres except
 481 germline cells from the 32- to 110-cell stage (Tomioka et al., 2002). We reasoned that, given its
 482 expression pattern, an upstream transcription factor regulating *Clone 22* expression could be present
 483 ubiquitously, including in germline cells. In our experiments, DMSO treatment, NC MO injection
 484 and GSK126 inhibitor treatment did not lead to ectopic *Clone 22* expression in germline cells (Figs.
 485 8Aa, b, c, B and S9). In contrast, knockdown of Pem resulted in ectopic expression of *Clone 22* in
 486 the germline at the 110-cell stage (19.4%, n = 36; Figs. 8Ad, B and S9). Furthermore, inhibition of
 487 H3K27me3 by the inhibitor treatment together with Pem knockdown resulted in significantly more
 488 embryos mis-expressing *Clone 22* in the germline (33.3%, n = 60; Figs. 8Ae, B and S9), indicating
 489 that H3K27me3 contributes to repressing *Clone 22* expression in the germline, although this

490 function could only be seen in the Pem knockdown background. These results suggest that *Clone 22*
 491 expression may be regulated by a ubiquitously expressed transcription factor(s) and that Pem and
 492 H3K27me3 suppress the outcome of this expression in the germline at the 110-cell stage.

493

494 3.8. pSer2-CTD and H3K27me3 levels are regulated independently of each other

495 In our final experiments, we examined whether there is a causal relationship between the
 496 regulation of pSer2-CTD and H3K27me3 levels since the timing of the upregulation of H3K27me3
 497 coincides with the decrease in Pem protein level (Fig. 2; Negishi et al., 2007). To this end, we
 498 examined whether Pem knockdown or GSK126 inhibitor treatment would affect the H3K27me3 or
 499 pSer2-CTD levels, respectively, at the 110-cell stage. Although Pem knockdown resulted in an
 500 increase in the pSer2-CTD level (Fig. 9A), it did not cause a significant change in the H3K27me3
 501 level (Fig. 9B). Likewise, the inhibitor treatment reduced the H3K27me3 level (Fig. 9C), but did not
 502 change the pSer2-CTD level significantly (Fig. 9D). These observations were confirmed by assessing
 503 the average intensities of fluorescent nuclear signals from confocal Z-stack images (Fig. 9A', B', C'
 504 and D'). Taken together, these data indicate that the levels of pSer2-CTD and H3K27me3 are
 505 regulated independently of each other.

506

507 4. Discussion

508 In this study, we present evidence that H3K27me3 and Pem play key roles in repressing somatic
 509 gene expression in the germline at the 110-cell stage. Repression of somatic gene expression at this
 510 stage of embryogenesis is crucial for further germline development since the germline is no longer in
 511 a state where transcription is quiescent after the Pem protein level and its contribution to
 512 transcriptional repression have declined (Negishi et al., 2007; Kumano et al., 2011) and zygotic gene
 513 expression for PGC differentiation commences (Miyaoku et al., 2018). Earlier in development, the
 514 germline is transcriptionally quiescent because of the function of a germ plasm factor, Pem (Kumano

515 et al., 2011; Shirae-Kurabayashi et al., 2011). Therefore, our findings suggest that H3K27me3 may be
 516 a factor to selectively repress somatic gene expression while germline genes are activated in the
 517 germline cells. Another important finding from the current study is that germline cells with Pem and
 518 H3K27me3 levels downregulated ectopically expressed their sister lineage tissue markers and muscle
 519 developmental genes and that this ectopic expression was dependent on a maternally localized muscle
 520 determinant, Macho-1. The muscle fate is shared with the germ cell fate until the last cell division
 521 completing germline segregation from all the somatic fates (Nishida, 1987). Therefore, this
 522 phenomenon may be a unique feature to ascidians, whose germline segregation is achieved by
 523 progressive asymmetric cell divisions during cell cleavage stages in early embryogenesis.

524

525 4.1. Low percentage of embryos showing ectopic somatic gene expression

526 In our studies, relatively few embryos showed ectopic *MA4* or *Snail* expression (Fig. 4). This
 527 may be due to insufficient Pem knockdown. Pem is known to regulate the posterior-specific cell
 528 division pattern (Negishi et al., 2007) in addition to repressing germline transcription (Kumano et
 529 al., 2011; Shirae-Kurabayashi et al., 2011). Thus, to identify germline cells at the 110-cell stage, it
 530 was necessary to limit the amount of injected Pem MO to a certain level. In fact, with the
 531 concentration of MO used in this study, Pem MO-injected embryos sometimes showed abnormal
 532 morphology (Fig. S7), and only a half of them showed an elevated level of pSer2-CTD at the
 533 110-cell stage (Fig. 2D). Accordingly, this limitation may have reduced the proportion of embryos
 534 with ectopic somatic gene expression in the germline, but the possibility also remains that there may
 535 be factors, other than Pem and H3K27me3 that repress somatic gene expression in germline cells,
 536 such as *Postplasmic/PEM* RNAs (Yoshida et al., 1996; Prodon et al., 2007; Makabe and Nishida,
 537 2012).

538

539 4.2. Preferential ectopic expression of muscle developmental genes in the germline

540 It was observed in the present study that, upon downregulation of H3K27me3 and Pem, muscle
541 developmental genes were mis-expressed in the germline, but other tissue-specific genes were not,
542 namely the notochord gene *Brachyury* (Fig. 5B), the nerve cord marker *ETR-1* (Fig. 5C) and the
543 heart precursor gene *Mesp* (Fig. 5A). We propose that this difference is due to a muscle
544 determinant, Macho-1, shared between the muscle B7.5 lineage and the germline, which are sister
545 lineages at the 110-cell stage. Ectopic expression of *Clone 22* in germline cells observed in this
546 study also supports the importance of suppressing the function of transcription factors present in the
547 sister lineage, not the muscle differentiation program *per se*. Previous studies on *C. elegans* showed
548 that depletion of P granules (the *C. elegans* version of germ granules) upregulated a large number of
549 genes involved in neuron and muscle differentiation in germline cells (Updike et al., 2014). While
550 the last somatic lineage that is separated from the germline (at the fourth division after fertilization)
551 is the muscle lineage (D lineage) in *C. elegans*, the majority of neurons originate from the sister
552 blastomere AB to the germline P1 at the 2-cell stage (Sulston et al., 1983). Importantly, *C. elegans*
553 embryos also segregate germline progressively from somatic lineages by successive asymmetric
554 cell divisions during cell cleavage stages, similarly to ascidian embryos. Therefore, with this
555 method of segregating the germline, embryos may have to actively prevent the sister-lineage
556 somatic program because of shared upstream transcription factors. Even DNA structures in the
557 genome could be changed progressively as germline is segregated from somatic lineages one cell
558 cycle after another to limit its transcriptional capability. However, in *C. elegans*, there are probably
559 other mechanisms than preventing the sister-lineage program.

560 It is suggested that *C. elegans* germline cells trans-differentiate into neuronal cells because the
561 neuronal fate is considered to be a ‘default’ fate (Kaneshiro et al., 2019). In *H. roretzi* embryos, the
562 nerve cord fate is also considered to be a default fate (Minokawa et al., 2001). However, as
563 mentioned above, the nerve cord marker gene *ETR-1* was not ectopically expressed in germline
564 cells deficient in Pem- and H3K27me3 (Fig. 5C). We speculate that this may be due to the presence
565 of Macho-1 in the germline. Previous research has shown that without Macho-1, *ETR-1* is

566 ectopically expressed in the posterior region of the embryo (Kobayashi et al., 2003), indicating that
 567 Macho-1 represses the nerve cord fate. The same could be also true for the notochord gene
 568 *Brachyury* since it, too, is ectopically expressed in the posterior region upon Macho-1 knockdown
 569 (Kobayashi et al., 2003). Therefore, it would be interesting to discover which kind of somatic genes
 570 are expressed in the germline cells from the triple downregulation of Pem, H3K27me3 and
 571 Macho-1 (Fig. 7C).

572 To our surprise, *Tbx6* was not ectopically expressed in germline cells deficient in Pem- and
 573 H3K27me3 (Fig. 6B). It is known to be a direct target of Macho-1 (Mitani et al., 1999; Kumano et
 574 al., 2014; Kugler et al., 2010; Yu et al., 2019), as also are *MA4* and *Snail* (Satou et al., 1995; Sawada
 575 et al., 2005; Tokuoka et al., 2018), and is required for muscle development (Mitani et al., 1999;
 576 Kumano et al., 2014; Kugler et al., 2010; Yu et al., 2019). The expression of *Tbx6* could require
 577 other factors, in addition to Macho-1, which are still repressed in the germline by other mechanisms
 578 than that involving Pem and H3K27me3. *Zic-r: b* and *Mrf* are shown to be required for the
 579 expression of *Ciona* orthologue of *Tbx6* at the 110-cell stage (Yu et al., 2019), although this
 580 regulation was observed only in muscle lineage cells other than B7.5.

581 Interestingly, the absence of ectopic *Tbx6* expression may explain why muscle
 582 trans-differentiation was incomplete and also why the heart marker *Mesp* was not ectopically
 583 expressed even though the heart is in the sister lineage to the germline shared with the muscle B7.5
 584 lineage at the 110-cell stage (Fig. 5D). In *C. intestinalis*, *Mesp* is known to be activated by the
 585 combined actions of *Tbx6* and *Lhx3* (Christiaen et al., 2009).

586

587 4.3. Impact of de-silencing somatic gene expression on germline and other lineage cells

588 In the current study, we were unable to determine by the expression analysis of the *ADP/ATP*
 589 *tranlocase* gene whether Pem- and H3K27me3-deficient germline cells retain germline features
 590 through later stages (Fig. 6C). There are many other germline-specific features of embryogenesis

known in ascidians which are also conserved in other animal species, such as: expression of other
 germline genes (Makabe et al., 2001; Miyaoku et al., 2018); perinuclear localization of Vasa protein
 (Shirae-Kurabayashi et al., 2006); cell division arrest (Shirae-Kurabayashi et al., 2006); and cell
 migration and incorporation into the gonads (Shirae-Kurabayashi et al., 2006; Takamura et al.,
 2002). Future experiments on these aspects will be required to better understand the impact of
 mis-regulation of germline transcription at the 110-cell stage on later germline cell development. In
 contrast, there is also the potential impact on the development of other lineage cells. One hypothesis
 is that germline silencing protects its sister lineage B7.5 cells from precocious FGF-dependent
 tissue induction (Davidson and Levine, 2003). The loss of endogenous *MA4* expression in B7.5
 observed in the present study (Fig. S7) could be due to such precocious induction. Although this
 hypothetical effect on B7.5 would occur during cell cleavage stages before the 110-cell stage and is
 only possible because ascidian germline is progressively segregated from somatic lineages by
 successive asymmetric divisions during the cleavage stages, it would be interesting to investigate
 whether or not PGC has an impact on the development of neighbouring somatic lineage cells at later
 stages.

606

607 4.4. An evolutionarily conserved transition: chromatin-based transcriptional repression relays
 608 repression by maternally localized factors

609 Our results suggest that H3K27me3 may be responsible for selective transcriptional repression
 610 of somatic genes even after germline zygotic gene expression begins. Interestingly, these later-stage
 611 germline cells showed both active (H3K4me3) and repressive (H3K27me3) chromatin marks
 612 simultaneously (Figs. 3 and S2, and Table S1). This is known as poised (bivalent) chromatin and is
 613 found at promoters of key developmental genes for possible function in the maintenance of germ cell
 614 identity (Robert et al., 2015). Therefore, poised chromatin could be a part of the mechanisms for the
 615 selective repression in ascidian germline cells.

616 A transition from mechanisms relying on maternally localized factors to those involving

617 chromatin-based regulation for transcriptional repression in the germline is also found in other
 618 organisms. In *C. elegans*, the P granule component transcriptional repressor PIE-1 becomes
 619 undetectable after the division of PGC P4 into Z2 and Z3 (Seydoux and Dunn, 1997). In these
 620 daughter cells, histone modifications associated with active transcription, such as H3K4me2/3,
 621 become specifically absent, but the same modifications remain at high levels in somatic cells
 622 (Schaner et al., 2003). In *Drosophila*, maternally localized germline repressor Pgc disappears during
 623 the stage 6-7 of embryogenesis (Hanyu-Nakamura et al., 2008) and only a low level of zygotic gene
 624 expression is detectable in germline cells until they begin to migrate at stage 9 (Zalokar, 1976; Van
 625 Doren et al., 1998; Martinho et al., 2004). However, mutation of Osa, a component of the Swi/Snf
 626 chromatin remodeling complex, causes precocious zygotic transcription in germline cells soon after
 627 Pgc disappears (Martinho et al., 2004). Thus, such a relay mechanism for germline transcriptional
 628 repression may be conserved across different animal species that rely on the germ plasm for
 629 germline development.

630

631

632 Acknowledgments

633 We are sincerely grateful to Prof. Hiroki Nishida at Osaka University for kindly offering us the
 634 plasmids for making *in situ* probes of *MA4*, *Clone 22*, *ETR-1* and *ADP/ATP translocase*. This work
 635 was supported by a Grant-in-Aid for Scientific Research (KAKENHI) 15K07071 from the Japan
 636 Society for the Promotion of Sciences, and by a Grant-in-Aid for Scientific Research (KAKENHI) on
 637 Innovative Areas, ‘Mechanisms regulating gamete formation in animals’ (16H01250), the Ministry of
 638 Education, Culture, Sports, Science and Technology, to GK. In addition, Tao Zheng would like to
 639 thank the China Scholarship Council (CSC) for supporting his stay in Japan.

640

641

642 Declarations of interest

643 None.

644

References

- 645 Batchelder, C., Dunn, M.A., Choy, B., Suh, Y., Cassie, C., Shim, E.Y., Shin, T.H., Mello, C.,
646 Seydoux, G., Blackwell, T.K., 1999. Transcriptional repression by the *Caenorhabditis elegans*
647 germ-line protein PIE-1. *Genes Dev.* 13, 202–212. <https://doi.org/10.1101/gad.13.2.202>
- 648 Brookes, E., Pombo, A., 2009. Modifications of RNA polymerase II are pivotal in regulating gene
649 expression states. *EMBO Rep.* 10, 1213–1219. <https://doi.org/10.1038/embor.2009.221>
- 650 Brunetti, R., Gissi, C., Pennati, R., Caicci, F., Gasparini, F., Manni, L., 2015. Morphological evidence
651 that the molecularly determined *Ciona intestinalis* type A and type B are different species: *Ciona*
652 *robusta* and *Ciona intestinalis*. *J. Zool. Syst. Evol. Res.* 53, 186–193.
653 <https://doi.org/10.1111/jzs.12101>
- 654 Christiaen, L., Stolfi, A., Davidson, B., Levine, M., 2009. Spatio-temporal intersection of Lhx3 and
655 Tbx6 defines the cardiac field through synergistic activation of Mesp. *Dev. Biol.* 328, 552–560.
656 <https://doi.org/10.1016/j.ydbio.2009.01.033>
- 657 Ciosk, R., DePalma, M., Priess, J.R., 2006. Translational Regulators Maintain Totipotency in the
658 *Caenorhabditis elegans* Germline. *Science* 311, 851–853.
659 <https://doi.org/10.1126/science.1122491>
- 660 Davidson, B., Levine, M., 2003. Evolutionary origins of the vertebrate heart: Specification of the
661 cardiac lineage in *Ciona intestinalis*. *Proc. Natl. Acad. Sci.* 100, 11469–11473.
662 <https://doi.org/10.1073/pnas.1634991100>
- 663 Fujiwara, S., Corbo, J.C., Levine, M., 1998. The snail repressor establishes a muscle/notochord
664 boundary in the *Ciona* embryo. *Development* 125, 2511–2520.
- 665 Gross-Thebing, T., Yigit, S., Pfeiffer, J., Reichman-Fried, M., Bandemer, J., Ruckert, C., Rathmer, C.,
666 Goudarzi, M., Stehling, M., Tarbashevich, K., Seggewiss, J., Raz, E., 2017. The Vertebrate
667 Protein Dead End Maintains Primordial Germ Cell Fate by Inhibiting Somatic Differentiation.
668 *Dev. Cell* 43, 704-715.e5. <https://doi.org/10.1016/j.devcel.2017.11.019>

- 669 Hanyu-Nakamura, K., Sonobe-Nojima, H., Tanigawa, A., Lasko, P., Nakamura, A., 2008. *Drosophila*
 670 Pgc protein inhibits P-TEFb recruitment to chromatin in primordial germ cells. *Nature* 451,
 671 730–733. <https://doi.org/10.1038/nature06498>
- 672 Hayashi, Y., Hayashi, M., Kobayashi, S., 2004. Nanos suppresses somatic cell fate in *Drosophila*
 673 germ line. *Proc. Natl. Acad. Sci.* 101, 10338–10342. <https://doi.org/10.1073/pnas.0401647101>
- 674 Heasman, J., Quarmby, J., Wylie, C.C., 1984. The mitochondrial cloud of *Xenopus* oocytes: The
 675 source of germinal granule material. *Dev. Biol.* 105, 458–469.
 676 [https://doi.org/10.1016/0012-1606\(84\)90303-8](https://doi.org/10.1016/0012-1606(84)90303-8)
- 677 Hibino, T., Nishikata, T., Nishida, H., 1998. Centrosome-attracting body: A novel structure closely
 678 related to unequal cleavages in the ascidian embryo. *Dev. Growth Differ.* 40, 85–95.
 679 <https://doi.org/10.1046/j.1440-169X.1998.t01-5-00010.x>
- 680 Hsin, J.-P., Manley, J.L., 2012. The RNA polymerase II CTD coordinates transcription and RNA
 681 processing. *Genes Dev.* 26, 2119–2137. <https://doi.org/10.1101/gad.200303.112>
- 682 Ikenishi, K., 1998. Germ plasm in *Caenorhabditis elegans*, *Drosophila* and *Xenopus*. *Dev. Growth
 683 Differ.* 40, 1–10. <https://doi.org/10.1046/j.1440-169X.1998.t01-4-00001.x>
- 684 Kaneshiro, K.R., Rechtsteiner, A., Strome, S., 2019. Sperm-inherited H3K27me3 impacts offspring
 685 transcription and development in *C. elegans*. *Nat. Commun.* 10.
 686 <https://doi.org/10.1038/s41467-019-09141-w>
- 687 Kaniskan, H.Ü., Martini, M.L., Jin, J., 2018. Inhibitors of Protein Methyltransferases and
 688 Demethylases. *Chem. Rev.* 118, 989–1068. <https://doi.org/10.1021/acs.chemrev.6b00801>
- 689 Kobayashi, K., Sawada, K., Yamamoto, H., Wada, S., Saiga, H., Nishida, H., 2003. Maternal macho-1
 690 is an intrinsic factor that makes cell response to the same FGF signal differ between mesenchyme
 691 and notochord induction in ascidian embryos. *Development* 130, 5179–5190.
 692 <https://doi.org/10.1242/dev.00732>

- 693 Kugler, J.E., Gazdoiu, S., Oda-Ishii, I., Passamanek, Y.J., Erives, A.J., Gregorio, A.D., 2010.
- 694 Temporal regulation of the muscle gene cascade by Macho1 and Tbx6 transcription factors in
695 *Ciona intestinalis*. *J. Cell Sci.* 123, 2453–2463. <https://doi.org/10.1242/jcs.066910>
- 696 Kumano, G., 2018. Microinjection of Exogenous DNA into Eggs of *Halocynthia roretzi*. *Adv. Exp.
697 Med. Biol.* 1029, 25–35. https://doi.org/10.1007/978-981-10-7545-2_4
- 698 Kumano, G., 2014. Taxon-Specific Maternal Factors for Germline Specification, in: Kondoh, H.,
699 Kuroiwa, A. (Eds.), *New Principles in Developmental Processes*. Springer Japan, Tokyo, pp.
700 3–11. https://doi.org/10.1007/978-4-431-54634-4_1
- 701 Kumano, G., Kawai, N., Nishida, H., 2010. Macho-1 regulates unequal cell divisions independently
702 of its function as a muscle determinant. *Dev. Biol.* 344, 284–292.
703 <https://doi.org/10.1016/j.ydbio.2010.05.013>
- 704 Kumano, G., Negoro, N., Nishida, H., 2014. Transcription factor Tbx6 plays a central role in fate
705 determination between mesenchyme and muscle in embryos of the ascidian, *Halocynthia roretzi*.
706 *Dev. Growth Differ.* 56, 310–322. <https://doi.org/10.1111/dgd.12133>
- 707 Kumano, G., Nishida, H., 2009. Patterning of an ascidian embryo along the anterior–posterior axis
708 through spatial regulation of competence and induction ability by maternally localized PEM.
709 *Dev. Biol.* 331, 78–88. <https://doi.org/10.1016/j.ydbio.2009.04.024>
- 710 Kumano, G., Takatori, N., Negishi, T., Takada, T., Nishida, H., 2011. A Maternal Factor Unique to
711 Ascidians Silences the Germline via Binding to P-TEFb and RNAP II Regulation. *Curr. Biol.* 21,
712 1308–1313. <https://doi.org/10.1016/j.cub.2011.06.050>
- 713 Kumar, S., Stecher, G., Tamura, K., 2016. MEGA7: Molecular Evolutionary Genetics Analysis
714 Version 7.0 for Bigger Datasets. *Mol. Biol. Evol.* 33, 1870–1874.
715 <https://doi.org/10.1093/molbev/msw054>
- 716 Kusakabe, T., 1995. Expression of larval-type muscle actin-encoding genes in the ascidian
717 *Halocynthia roretzi*. *Gene* 153, 215–218. [https://doi.org/10.1016/0378-1119\(94\)00762-H](https://doi.org/10.1016/0378-1119(94)00762-H)

- 718 Kusakabe, T., Suzuki, J., Saiga, H., Jeffery, W.R., Makabe, K.W., Satoh, N., 1991. Temporal and
 719 Spatial Expression of a Muscle Actin Gene during Embryogenesis of the Ascidian *Halocynthia*
 720 *roretzi*. Dev. Growth Differ. 33, 227–234. <https://doi.org/10.1111/j.1440-169X.1991.00227.x>
- 721 Lai, F., Singh, A., King, M.L., 2012. *Xenopus* Nanos1 is required to prevent endoderm gene
 722 expression and apoptosis in primordial germ cells. Development 139, 1476–1486.
 723 <https://doi.org/10.1242/dev.079608>
- 724 Lee, T.I., Jenner, R.G., Boyer, L.A., Guenther, M.G., Levine, S.S., Kumar, R.M., Chevalier, B.,
 725 Johnstone, S.E., Cole, M.F., Isono, K., Koseki, H., Fuchikami, T., Abe, K., Murray, H.L., Zucker,
 726 J.P., Yuan, B., Bell, G.W., Herbolzheimer, E., Hannett, N.M., Sun, K., Odom, D.T., Otte, A.P.,
 727 Volkert, T.L., Bartel, D.P., Melton, D.A., Gifford, D.K., Jaenisch, R., Young, R.A., 2006. Control
 728 of Developmental Regulators by Polycomb in Human Embryonic Stem Cells. Cell 125,
 729 301–313. <https://doi.org/10.1016/j.cell.2006.02.043>
- 730 Mahowald, A.P., 2001. Assembly of the *Drosophila* germ plasm, in: International Review of
 731 Cytology, Cell Lineage and Embryo Patterning. Academic Press, pp. 187–213.
 732 [https://doi.org/10.1016/S0074-7696\(01\)03007-8](https://doi.org/10.1016/S0074-7696(01)03007-8)
- 733 Makabe, K.W., Fujiwara, S., Saiga, H., Satoh, N., 1990. Specific expression of myosin heavy chain
 734 gene in muscle lineage cells of the ascidian embryo. Roux's Arch. Dev. Biol. 199, 307–313.
 735 <https://doi.org/10.1007/BF01709509>
- 736 Makabe, K.W., Kawashima, T., Kawashima, S., Minokawa, T., Adachi, A., Kawamura, H., Ishikawa,
 737 H., Yasuda, R., Yamamoto, H., Kondoh, K., Arioka, S., Sasakura, Y., Kobayashi, A., Yagi, K.,
 738 Shojima, K., Kondoh, Y., Kido, S., Tsujinami, M., Nishimura, N., Takahashi, M., Nakamura, T.,
 739 Kanehisa, M., Ogasawara, M., Nishikata, T., Nishida, H., 2001. Large-scale cDNA analysis of
 740 the maternal genetic information in the egg of *Halocynthia roretzi* for a gene expression catalog
 741 of ascidian development. Development 128, 2555–2567.

- 742 Makabe, K.W., Nishida, H., 2012. Cytoplasmic localization and reorganization in ascidian eggs: role
 743 of postplasmic/PEM RNAs in axis formation and fate determination. Wiley Interdiscip. Rev.
 744 Dev. Biol. 1, 501–518. <https://doi.org/10.1002/wdev.54>
- 745 Makabe, K.W., Satoh, N., 1989. Temporal Expression of Myosin Heavy Chain Gene during Ascidian
 746 Embryogenesis. Dev. Growth Differ. 31, 71–77.
 747 <https://doi.org/10.1111/j.1440-169X.1989.00071.x>
- 748 Margueron, R., Reinberg, D., 2011. The Polycomb complex PRC2 and its mark in life. Nature 469,
 749 343–349. <https://doi.org/10.1038/nature09784>
- 750 Martinho, R.G., Kunwar, P.S., Casanova, J., Lehmann, R., 2004. A Noncoding RNA Is Required for
 751 the Repression of RNAPolII-Dependent Transcription in Primordial Germ Cells. Curr. Biol. 14,
 752 159–165. <https://doi.org/10.1016/j.cub.2003.12.036>
- 753 McCabe, M.T., Ott, H.M., Ganji, G., Korenchuk, S., Thompson, C., Van Aller, G.S., Liu, Y., Graves,
 754 A.P., Iii, A.D.P., Diaz, E., LaFrance, L.V., Mellinger, M., Duquenne, C., Tian, X., Kruger, R.G.,
 755 McHugh, C.F., Brandt, M., Miller, W.H., Dhanak, D., Verma, S.K., Tummino, P.J., Creasy, C.L.,
 756 2012. EZH2 inhibition as a therapeutic strategy for lymphoma with EZH2-activating mutations.
 757 Nature 492, 108–112. <https://doi.org/10.1038/nature11606>
- 758 Meedel, T.H., Crowther, R.J., Whittaker, J.R., 1987. Determinative properties of muscle lineages in
 759 ascidian embryos. Development 100, 245–260.
- 760 Minokawa, T., Yagi, K., Makabe, K.W., Nishida, H., 2001. Binary specification of nerve cord and
 761 notochord cell fates in ascidian embryos. Development 128, 2007–2017.
- 762 Mitani, Y., Takahashi, H., Satoh, N., 2001. Regulation of the muscle-specific expression and function
 763 of an ascidian T-box gene, As-T2. Development 128, 3717–3728.
- 764 Mitani, Y., Takahashi, H., Satoh, N., 1999. An ascidian T-box gene As-T2 is related to the Tbx6
 765 subfamily and is associated with embryonic muscle cell differentiation. Dev. Dyn. 215, 62–68.
 766 [https://doi.org/10.1002/\(SICI\)1097-0177\(199905\)215:1<62::AID-DVDY7>3.0.CO;2-X](https://doi.org/10.1002/(SICI)1097-0177(199905)215:1<62::AID-DVDY7>3.0.CO;2-X)

- 767 Miya, T., Makabe, K.W., Satoh, N., 1994. Expression of a Gene for Major Mitochondrial Protein,
 768 ADP/ATP Translocase, during Embryogenesis in the Ascidian *Halocynthia roretzi*. Dev. Growth
 769 Differ. 36, 39–48. <https://doi.org/10.1111/j.1440-169X.1994.00039.x>
- 770 Miyaoku, K., Nakamoto, A., Nishida, H., Kumano, G., 2018. Control of Pem protein level by
 771 localized maternal factors for transcriptional regulation in the germline of the ascidian,
 772 *Halocynthia roretzi*. PLOS ONE 13, e0196500. <https://doi.org/10.1371/journal.pone.0196500>
- 773 Nakamura, A., Seydoux, G., 2008. Less is more: specification of the germline by transcriptional
 774 repression. Development 135, 3817–3827. <https://doi.org/10.1242/dev.022434>
- 775 Nakamura, A., Shirae-Kurabayashi, M., Hanyu-Nakamura, K., 2010. Repression of early zygotic
 776 transcription in the germline. Curr. Opin. Cell Biol. 22, 709–714.
 777 <https://doi.org/10.1016/j.ceb.2010.08.012>
- 778 Nakamura, Y., Makabe, K.W., Nishida, H., 2005. POPK-1/Sad-1 kinase is required for the proper
 779 translocation of maternal mRNAs and putative germ plasm at the posterior pole of the ascidian
 780 embryo. Development 132, 4731–4742. <https://doi.org/10.1242/dev.02049>
- 781 Negishi, T., Takada, T., Kawai, N., Nishida, H., 2007. Localized PEM mRNA and Protein Are
 782 Involved in Cleavage-Plane Orientation and Unequal Cell Divisions in Ascidians. Curr. Biol. 17,
 783 1014–1025. <https://doi.org/10.1016/j.cub.2007.05.047>
- 784 Nishida, H., 1987. Cell lineage analysis in ascidian embryos by intracellular injection of a tracer
 785 enzyme. III. Up to the tissue restricted stage. Dev. Biol. 121, 526–541.
 786 [https://doi.org/10.1016/0012-1606\(87\)90188-6](https://doi.org/10.1016/0012-1606(87)90188-6)
- 787 Nishida, H., 1986. Cell Division Pattern during Gastrulation of the Ascidian, *Halocynthia roretzi*.
 788 Dev. Growth Differ. 28, 191–201. <https://doi.org/10.1111/j.1440-169X.1986.00191.x>
- 789 Nishida, H., Sawada, K., 2001. macho-1 encodes a localized mRNA in ascidian eggs that specifies
 790 muscle fate during embryogenesis. Nature 409, 724. <https://doi.org/10.1038/35055568>

- 791 Nishikata, T., Hibino, T., Nishida, H., 1999. The Centrosome-Attracting Body, Microtubule System,
 792 and Posterior Egg Cytoplasm Are Involved in Positioning of Cleavage Planes in the Ascidian
 793 Embryo. *Dev. Biol.* 209, 72–85. <https://doi.org/10.1006/dbio.1999.9244>
- 794 Pae, J., Cinalli, R.M., Marzio, A., Pagano, M., Lehmann, R., 2017. GCL and CUL3 Control the
 795 Switch between Cell Lineages by Mediating Localized Degradation of an RTK. *Dev. Cell* 42,
 796 130-142.e7. <https://doi.org/10.1016/j.devcel.2017.06.022>
- 797 Prodon, F., Yamada, L., Shirae-Kurabayashi, M., Nakamura, Y., Sasakura, Y., 2007.
 798 Postplasmic/PEM RNAs: A class of localized maternal mRNAs with multiple roles in cell
 799 polarity and development in ascidian embryos. *Dev. Dyn.* 236, 1698–1715.
 800 <https://doi.org/10.1002/dvdy.21109>
- 801 Prokopuk, L., Stringer, J.M., Hogg, K., Elgass, K.D., Western, P.S., 2017. PRC2 is required for
 802 extensive reorganization of H3K27me3 during epigenetic reprogramming in mouse fetal germ
 803 cells. *Epigenetics Chromatin* 10, 7. <https://doi.org/10.1186/s13072-017-0113-9>
- 804 Robert, V.J., Garvis, S., Palladino, F., 2015. Repression of somatic cell fate in the germline. *Cell. Mol.
 805 Life Sci.* 72, 3599–3620. <https://doi.org/10.1007/s00018-015-1942-y>
- 806 Sasakura, Y., Ogasawara, M., Makabe, K.W., 2000. Two pathways of maternal RNA localization at
 807 the posterior-vegetal cytoplasm in early ascidian embryos. *Dev. Biol.* 220, 365–378.
 808 <https://doi.org/10.1006/dbio.2000.9626>
- 809 Satoh Noriyuki, Rokhsar Daniel, Nishikawa Teruaki, 2014. Chordate evolution and the three-phylum
 810 system. *Proc. R. Soc. B Biol. Sci.* 281, 20141729. <https://doi.org/10.1098/rspb.2014.1729>
- 811 Satou, Y., Imai, K.S., Satoh, N., 2004. The ascidian *Mesp* gene specifies heart precursor cells.
 812 *Development* 131, 2533–2541. <https://doi.org/10.1242/dev.01145>
- 813 Satou, Y., Kusakabe, T., Araki, L., Satoh, N., 1995. Timing of initiation of muscle-specific gene
 814 expression in the ascidian embryo precedes that of developmental fate restriction in lineage cells.
 815 *Dev. Growth Differ.* 37, 319–327. <https://doi.org/10.1046/j.1440-169X.1995.t01-2-00010.x>

- 816 Satou, Y., Yagi, K., Imai, K.S., Yamada, L., Nishida, H., Satoh, N., 2002. macho-1-related genes in
 817 *Ciona* embryos. Dev. Genes Evol. 212, 87–92. <https://doi.org/10.1007/s00427-002-0218-3>
- 818 Sawada, K., Fukushima, Y., Nishida, H., 2005. Macho-1 functions as transcriptional activator for
 819 muscle formation in embryos of the ascidian *Halocynthia roretzi*. Gene Expr. Patterns 5,
 820 429–437. <https://doi.org/10.1016/j.modgep.2004.09.003>
- 821 Schaner, C.E., Deshpande, G., Schedl, P.D., Kelly, W.G., 2003. A Conserved Chromatin Architecture
 822 Marks and Maintains the Restricted Germ Cell Lineage in Worms and Flies. Dev. Cell 5,
 823 747–757.
- 824 Seydoux, G., Dunn, M.A., 1997. Transcriptionally repressed germ cells lack a subpopulation of
 825 phosphorylated RNA polymerase II in early embryos of *Caenorhabditis elegans* and *Drosophila*
 826 *melanogaster*. Development 124, 2191–2201.
- 827 Shirae-Kurabayashi, M., Matsuda, K., Nakamura, A., 2011. Ci-Pem-1 localizes to the nucleus and
 828 represses somatic gene transcription in the germline of *Ciona intestinalis* embryos. Development
 829 138, 2871–2881. <https://doi.org/10.1242/dev.058131>
- 830 Shirae-Kurabayashi, M., Nishikata, T., Takamura, K., Tanaka, K.J., Nakamoto, C., Nakamura, A.,
 831 2006. Dynamic redistribution of vasa homolog and exclusion of somatic cell determinants during
 832 germ cell specification in *Ciona intestinalis*. Development 133, 2683–2693.
 833 <https://doi.org/10.1242/dev.02446>
- 834 Simon, J.A., Kingston, R.E., 2009. Mechanisms of Polycomb gene silencing: knowns and unknowns.
 835 Nat. Rev. Mol. Cell Biol. 10, 697–708. <https://doi.org/10.1038/nrm2763>
- 836 Spencer, W.C., Zeller, G., Watson, J.D., Henz, S.R., Watkins, K.L., McWhirter, R.D., Petersen, S.,
 837 Sreedharan, V.T., Widmer, C., Jo, J., Reinke, V., Petrella, L., Strome, S., Von Stetina, S.E., Katz,
 838 M., Shaham, S., Rätsch, G., Miller, D.M., 2011. A spatial and temporal map of *C. elegans* gene
 839 expression. Genome Res. 21, 325–341. <https://doi.org/10.1101/gr.114595.110>

- 840 Strome, S., Lehmann, R., 2007. Germ Versus Soma Decisions: Lessons from Flies and Worms.
 841 Science 316, 392–393. <https://doi.org/10.1126/science.1140846>
- 842 Strome, S., Updike, D., 2015. Specifying and protecting germ cell fate. Nat. Rev. Mol. Cell Biol. 16,
 843 406–416. <https://doi.org/10.1038/nrm4009>
- 844 Strome, S., Wood, W.B., 1982. Immunofluorescence visualization of germ-line-specific cytoplasmic
 845 granules in embryos, larvae, and adults of *Caenorhabditis elegans*. Proc. Natl. Acad. Sci. 79,
 846 1558–1562. <https://doi.org/10.1073/pnas.79.5.1558>
- 847 Sulston, J.E., Schierenberg, E., White, J.G., Thomson, J.N., 1983. The embryonic cell lineage of the
 848 nematode *Caenorhabditis elegans*. Dev. Biol. 100, 64–119.
 849 [https://doi.org/10.1016/0012-1606\(83\)90201-4](https://doi.org/10.1016/0012-1606(83)90201-4)
- 850 Takamura, K., Fujimura, M., Yamaguchi, Y., 2002. Primordial germ cells originate from the
 851 endodermal strand cells in the ascidian *Ciona intestinalis*. Dev. Genes Evol. 212, 11–18.
 852 <https://doi.org/10.1007/s00427-001-0204-1>
- 853 Tokuoka, M., Kobayashi, K., Satou, Y., 2018. Distinct regulation of Snail in two muscle lineages of
 854 the ascidian embryo achieves temporal coordination of muscle development. Development 145,
 855 dev163915. <https://doi.org/10.1242/dev.163915>
- 856 Tokuoka, M., Kumano, G., Nishida, H., 2007. FGF9/16/20 and Wnt-5 α signals are involved in
 857 specification of secondary muscle fate in embryos of the ascidian, *Halocynthia roretzi*. Dev.
 858 Genes Evol. 217, 515–527. <https://doi.org/10.1007/s00427-007-0160-5>
- 859 Tomioka, M., Miya, T., Nishida, H., 2002. Repression of Zygotic Gene Expression in the Putative
 860 Germline Cells in Ascidian Embryos. Zoolog. Sci. 19, 49–55. <https://doi.org/10.2108/zsj.19.49>
- 861 Treen, N., Heist, T., Wang, W., Levine, M., 2018. Depletion of Maternal Cyclin B3 Contributes to
 862 Zygotic Genome Activation in the *Ciona* Embryo. Curr. Biol. 28, 1150-1156.e4.
 863 <https://doi.org/10.1016/j.cub.2018.02.046>

- 864 Updike, D.L., Knutson, A.K., Egelhofer, T.A., Campbell, A.C., Strome, S., 2014. Germ-Granule
 865 Components Prevent Somatic Development in the *C. elegans* Germline. Curr. Biol. 24, 970–975.
 866 <https://doi.org/10.1016/j.cub.2014.03.015>
- 867 Van Doren, M., Williamson, A.L., Lehmann, R., 1998. Regulation of zygotic gene expression in
 868 *Drosophila* primordial germ cells. Curr. Biol. CB 8, 243–246.
 869 [https://doi.org/10.1016/S0960-9822\(98\)70091-0](https://doi.org/10.1016/S0960-9822(98)70091-0)
- 870 Wada, S., Katsuyama, Y., Yasugi, S., Saiga, H., 1995. Spatially and temporally regulated expression
 871 of the LIM class homeobox gene Hrlim suggests multiple distinct functions in development of
 872 the ascidian, *Halocynthia roretzi*. Mech. Dev. 51, 115–126.
 873 [https://doi.org/10.1016/0925-4773\(95\)00359-9](https://doi.org/10.1016/0925-4773(95)00359-9)
- 874 Wada, S., Saiga, H., 1999. Cloning and embryonic expression of Hrsna, a snail family gene of the
 875 ascidian *Halocynthia roretzi*: Implication in the origins of mechanisms for mesoderm
 876 specification and body axis formation in chordates. Dev. Growth Differ. 41, 9–18.
 877 <https://doi.org/10.1046/j.1440-169x.1999.00408.x>
- 878 Yagi, K., Makabe, K., 2001. Isolation of an early neural maker gene abundantly expressed in the
 879 nervous system of the ascidian, *Halocynthia roretzi*. Dev. Genes Evol. 211, 49–53.
 880 <https://doi.org/10.1007/s004270000118>
- 881 Yagi, K., Satoh, N., Satou, Y., 2004. Identification of downstream genes of the ascidian muscle
 882 determinant gene Ci-macho1. Dev. Biol. 274, 478–489.
 883 <https://doi.org/10.1016/j.ydbio.2004.07.013>
- 884 Yasuo, H., Satoh, N., 1998. Conservation of the Developmental Role of Brachyuryin Notochord
 885 Formation in a Urochordate, the Ascidian *Halocynthia roretzi*. Dev. Biol. 200, 158–170.
 886 <https://doi.org/10.1006/dbio.1998.8958>
- 887 Yoshida, S., Marikawa, Y., Satoh, N., 1996. Posterior end mark, a novel maternal gene encoding a
 888 localized factor in the ascidian embryo. Development 122, 2005–2012.

- 889 Yu, D., Oda-Ishii, I., Kubo, A., Satou, Y., 2019. The regulatory pathway from genes directly activated
890 by maternal factors to muscle structural genes in ascidian embryos. Development 146,
891 dev173104. <https://doi.org/10.1242/dev.173104>
- 892 Zalokar, M., 1976. Autoradiographic study of protein and RNA formation during early development
893 of *Drosophila* eggs. Dev. Biol. 49, 425–437.

894

895

896 Figures

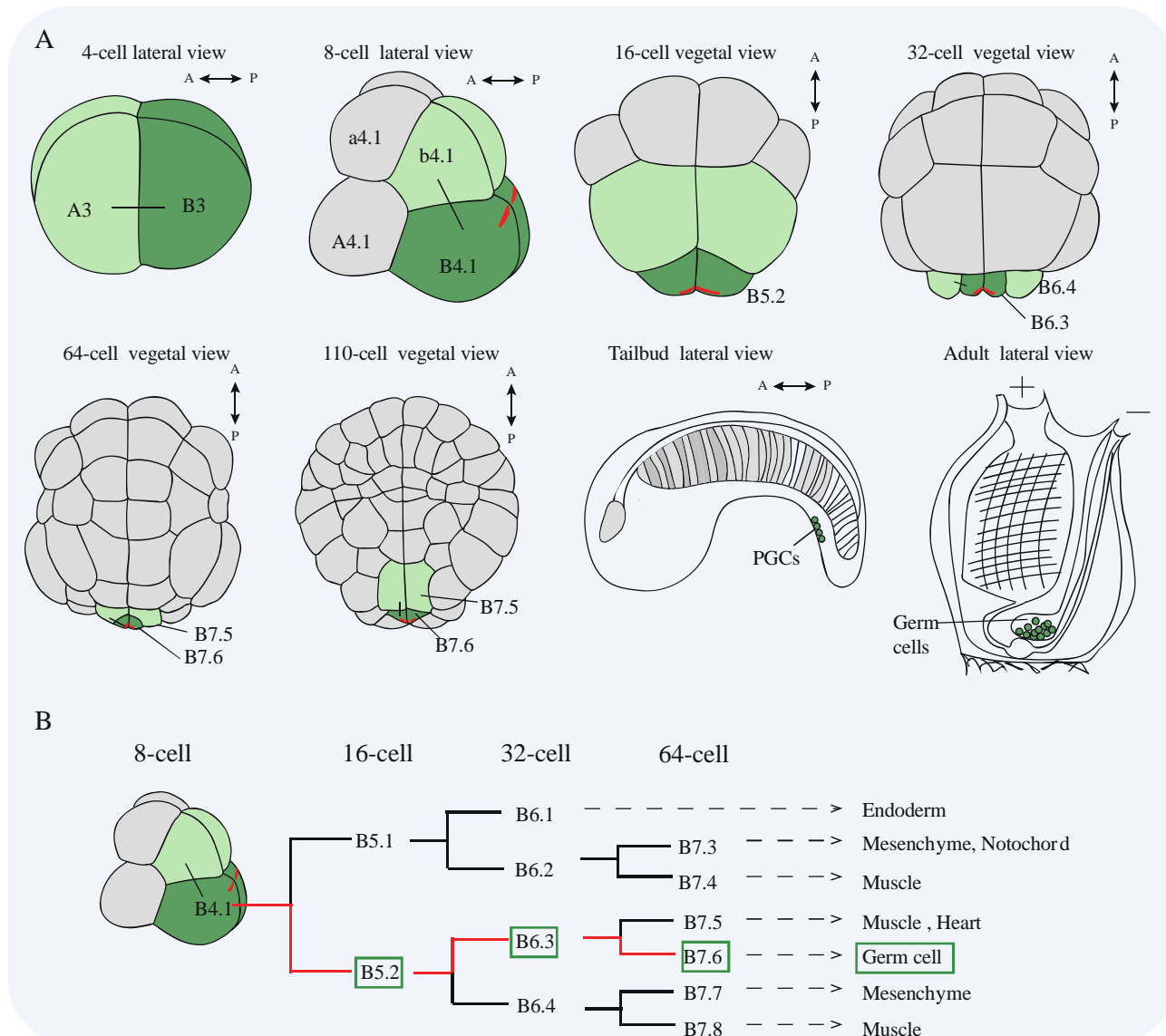
897
898

Fig. 1. Germline segregation in ascidians. (A) Schematic diagrams of ascidian embryos and an adult with germline cells indicated in dark green. Stages and views from which embryos and adult are viewed are indicated at the top of each cartoon. Germline cells during the cleavage stages (B4.1 at the 8-, B5.2 at the 16-, B6.3 at the 32-, and B7.6 at the 64- and 110-cell stages) are progressively segregated from sister somatic cells (light green) by mean of unequal cell divisions. Sister cells are connected by black lines. The ascidian germ plasm CAB is shown as red lines and is inherited by the germline cells, the most posterior pair of blastomeres. PGCs at the tailbud stage (dark green) are located close to the tip of the tail, and after metamorphosis are preserved and differentiated in the gonad of the adult animal. Abbreviations: A, anterior; P, posterior. (B) Cell lineage during ascidian

908 embryogenesis. The red line indicates the germline and the inheritance of the germ plasm by
909 germline cells (enclosed in green boxes).

910

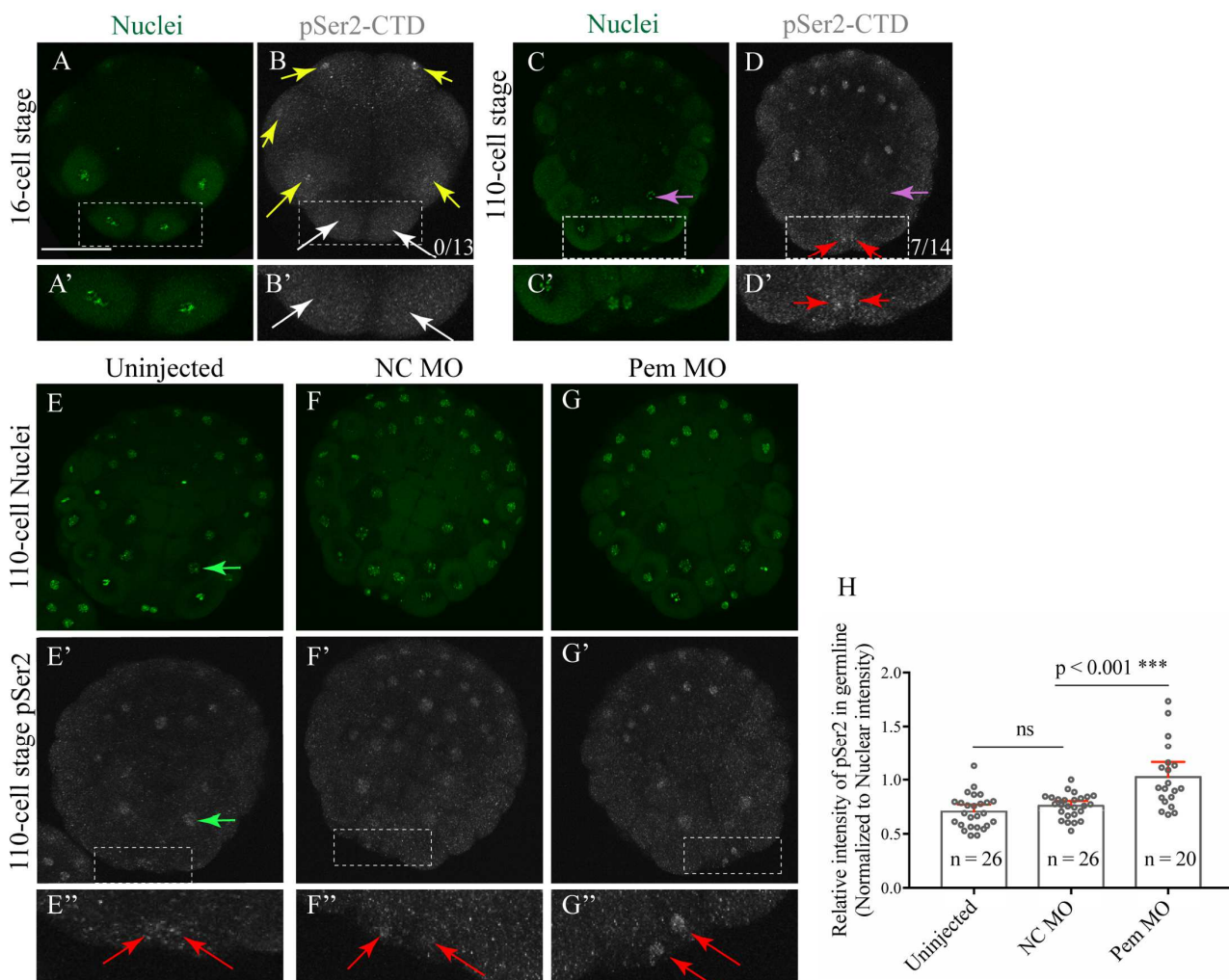
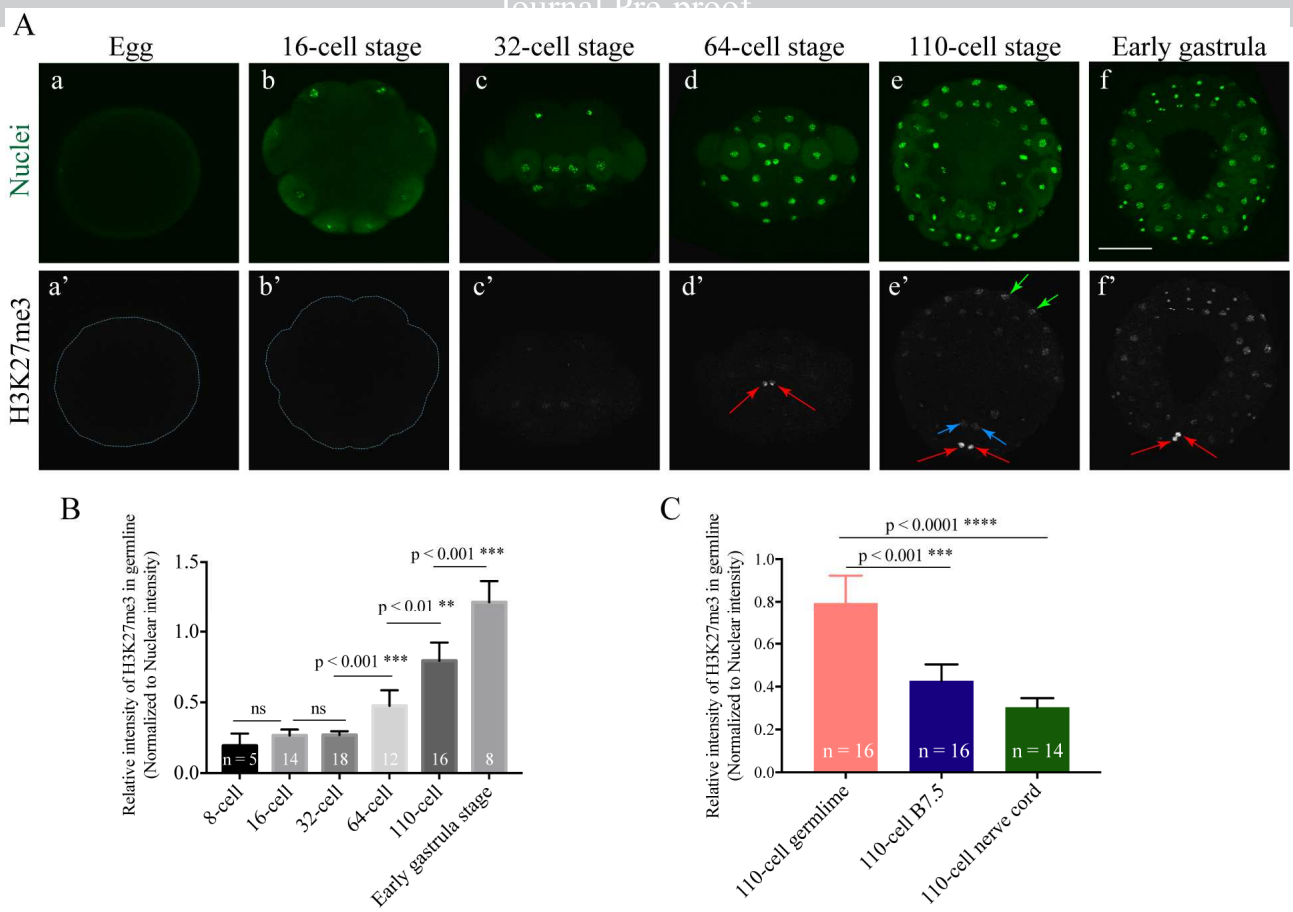
911
912

Fig. 2. Pem represses pSer2-CTD of RNAPII in the germline at the 110-cell stage. Immunostaining of the 16-cell stage (B) and 110-cell stage (D, E', F', G') embryos with the H5 antibody against pSer2-CTD of RNAPII. All nuclei were stained with SYTOX green (A, C, E, F, G). Vegetal hemispheres of representative embryos are shown with anterior up in the confocal Z-stack maximum projection (A, B, C, D, E, E', F, F', G, G'). Numbers in the lower right corner of the panels in B and D show the numbers of embryos with positive germline pSer2-CTD. Yellow arrows in B indicate positive pSer2-CTD signals in somatic nuclei at the 16-cell stage. White and red arrows indicate negative and positive pSer2-CTD signals, respectively, in germline nuclei (B, B', D, D', E'', F'', G''). Purple arrows in C and D indicate a somatic cell undergoing cell division, where pSer2-CTD was not observed. Green arrows in E and E' indicate the same somatic cell of a different embryo as that indicated by purple arrows in C and D, but with positive pSer2-CTD, and not undergoing cell division. (A', B', C', D', E'', F'', G'') Higher magnification of the posterior

925 regions enclosed by the white-dotted boxes in A, B, C, D, E', F' and G'. Scale bar, 100 µm. (H)

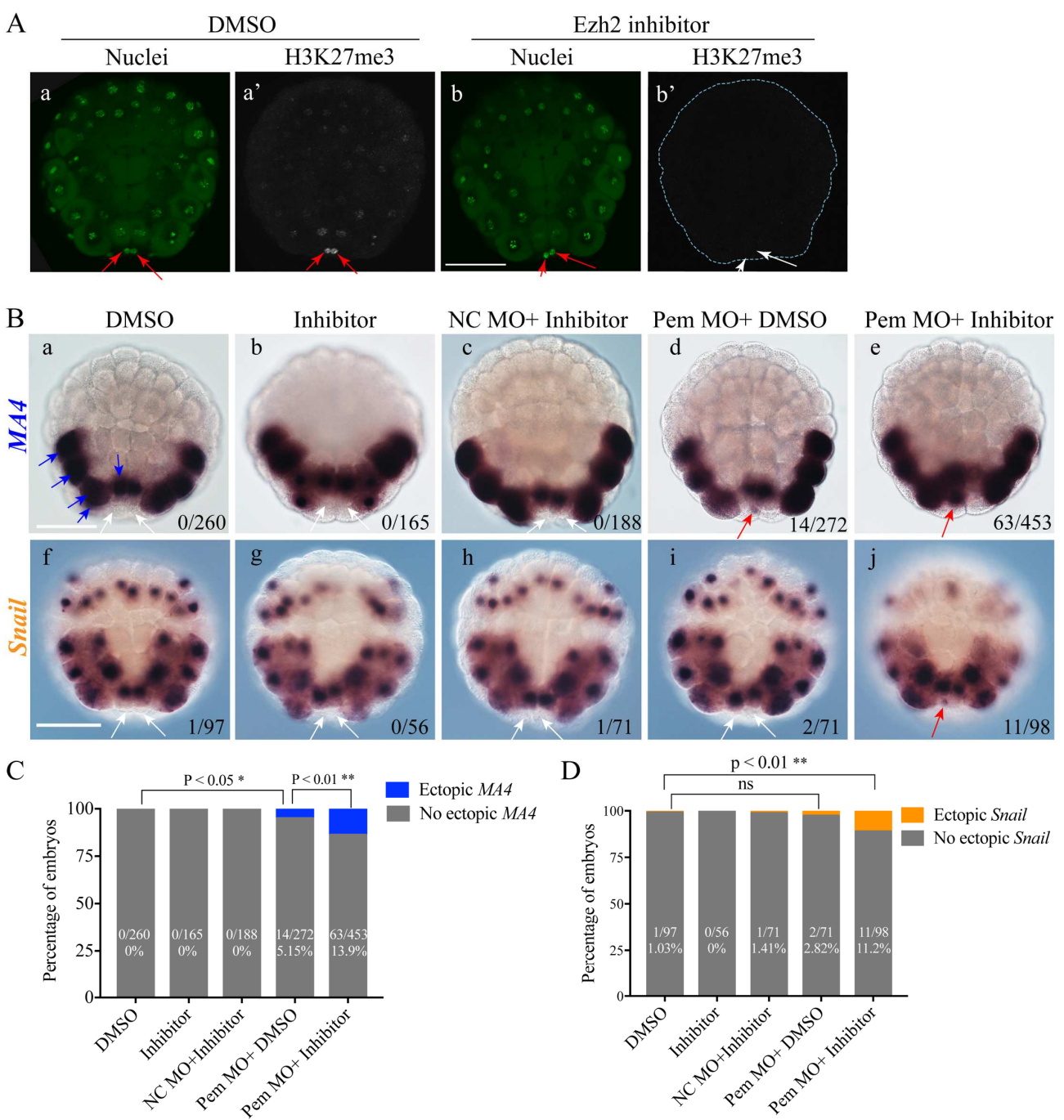
926 Quantification of fluorescent signal intensities for pSer2-CTD in the germline nuclei of embryos in
927 E', F', G'. The vertical scale indicates the pSer2-CTD signal intensity relative to that of SYTOX
928 green. Each circle represents a quantified value of each germline cell. The numbers of cells
929 examined are shown on the bar boxes. Differences in the relative intensity were statistically
930 analyzed by the Mann-Whitney U test. ns, no significant difference. Error bars (red) indicate 95%
931 confidence intervals.



932
933 Fig. 3. H3K27me3 is enriched in later embryonic germline cells of *H. roretzii*. (Aa'-f')

934 Immunostaining of H3K27me3 in embryos at different stages. All nuclei were stained with SYTOX
935 green (Aa-f). Vegetal views with anterior up are shown for the 16-cell (b, b') and 110-cell (e, e')
936 stages and early gastrula (f, f'). Posterior views are shown for 32- (c, c') and 64-cell (d, d') stage
937 embryos. Red arrows indicate positive H3K27me3 signals in the germline cells, while blue and
938 green arrows indicate B7.5 and nerve cord (A8.8, A8.15) cells, respectively. Scale bar, 100 μ m. (B)
939 Quantification of H3K27me3 fluorescent signal intensities in the germline nuclei of embryos from
940 8-cell to early gastrula stages. (C) Quantification of H3K27me3 fluorescent signal intensities in the
941 nuclei of the germline, B7.5, and nerve cord (A8.8 and A8.15) cells in 110-cell stage embryos. (B,
942 C) The vertical scales indicate the relative H3K27me3 signal intensity normalized to the SYTOX
943 nuclear staining. The numbers on the column bars indicate the numbers of blastomeres measured.
944 Differences in the H3K27me3 signal intensities between different categories were statistically
945 analyzed by the Mann-Whitney U test. ns, no significant difference. Error bars indicate 95%
946 confidence intervals.

948



949

950

951 Fig. 4. *MA4* and *Snail* are ectopically expressed in the germline. Vegetal views with anterior up. (A)

952 H3K27me3 is markedly decreased in embryos treated with the EZH2 inhibitor GSK126. Nuclei

953 were stained with SYTOX green (a, b). Immunostaining of H3K27me3 in the 110-cell stage

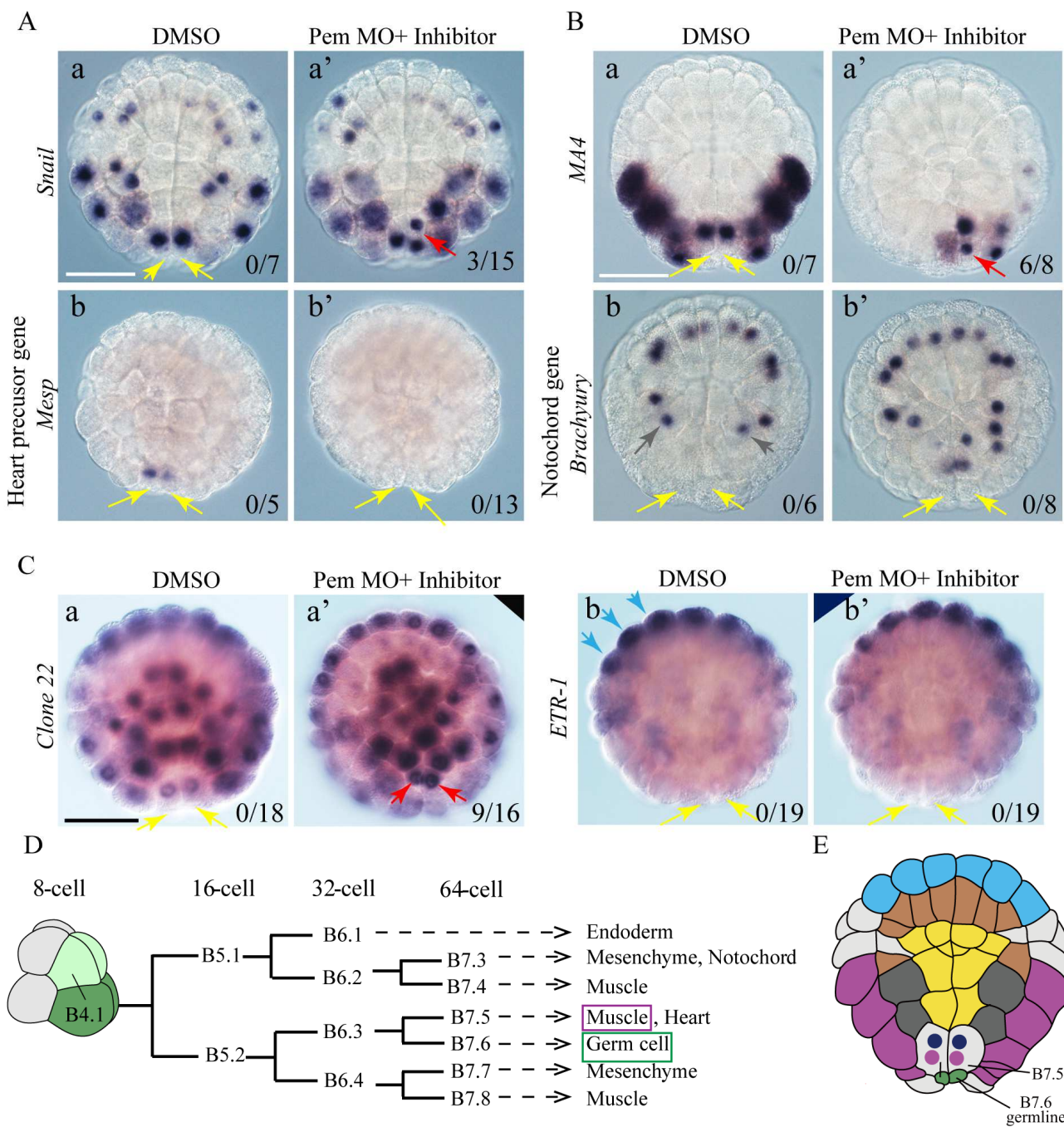
954 embryos treated with DMSO (a') and the EZH2 inhibitor (b'). Red arrows indicate the position of

955 germline nuclei (a, b) and positive signals for H3K27me3 in germline cells (a'). White arrows

956 indicate negative H3K27me3 signal in germline cells (b'). The dotted line in (b') outlines the

957 embryo. Scale bar, 100 μ m. (B) Detection of *MA4* (a-e) and *Snail* (f-j) expression by whole-mount
958 *in situ* hybridization after different treatments (shown above each image). Vegetal views with
959 anterior up. White and red arrows indicate the absence and presence, respectively, of ectopic gene
960 expression in germline cells. Blue arrows indicate endogenous *MA4* gene expression in each left
961 lateral member of five paired muscle cells. The number in the right bottom corner of each image
962 represents that of embryos showing ectopic gene expression in the germline. Scale bar, 100 μ m. (C,
963 D) The proportion of embryos showing ectopic *MA4* (C) and *Snail* (D) expression. The vertical
964 scale indicates the percentage of embryos with (colored) or without (gray) ectopic *MA4* (C) or *Snail*
965 (D) expression in the germline with the actual percentage value written on each bar. Results of
966 statistical analysis determined by two-tailed Fisher's Exact Test are shown above the bars (see Figs.
967 S6 and S7 for further details). ns, no significant difference.

968



969

970

Fig. 5. *Mesp*, *Brachyury*, and *ETR-I* do not show ectopic expression in embryos lacking Pem and H3K27me3. Vegetal views with anterior up. Detection of *Snail* and *Mesp* (A), *MA4* and *Brachyury* (B), *Clone 22* and *ETR-I* (C) expression at the 110-cell stage by whole-mount *in situ* hybridization in DMSO-treated control and Pem- and H3K27me3-deficient embryos. Note that 46.2% of embryos without Pem and H3K27me3 lost endogenous *Mesp* expression. Red and yellow arrows indicate presence or absence, respectively, of ectopic gene expression in the germline. Gray arrows in B indicate *Brachyury* signals in mesoderm cells. Blue arrows in C indicate *ETR-I* expression in

978 nerve cord cells. The figures in the bottom right corner of each image state the number of embryos
979 with ectopic gene expression in the germline. Scale bars, 100 μm . (D) B4.1 cell lineage during *H.*
980 *roretzi* embryogenesis. (E) Cartoon of the vegetal hemisphere of the 110-cell stage embryo showing
981 cell lineage. Green, germline cells B7.6; purple, primary muscle; gray, mesenchyme; yellow,
982 endoderm; brown, notochord; light blue, nerve cord. The fate of B7.5 at the 110-cell stage has not
983 been restricted to one fate and gives rise to primary muscle (purple dot) and heart (dark blue dot).

984

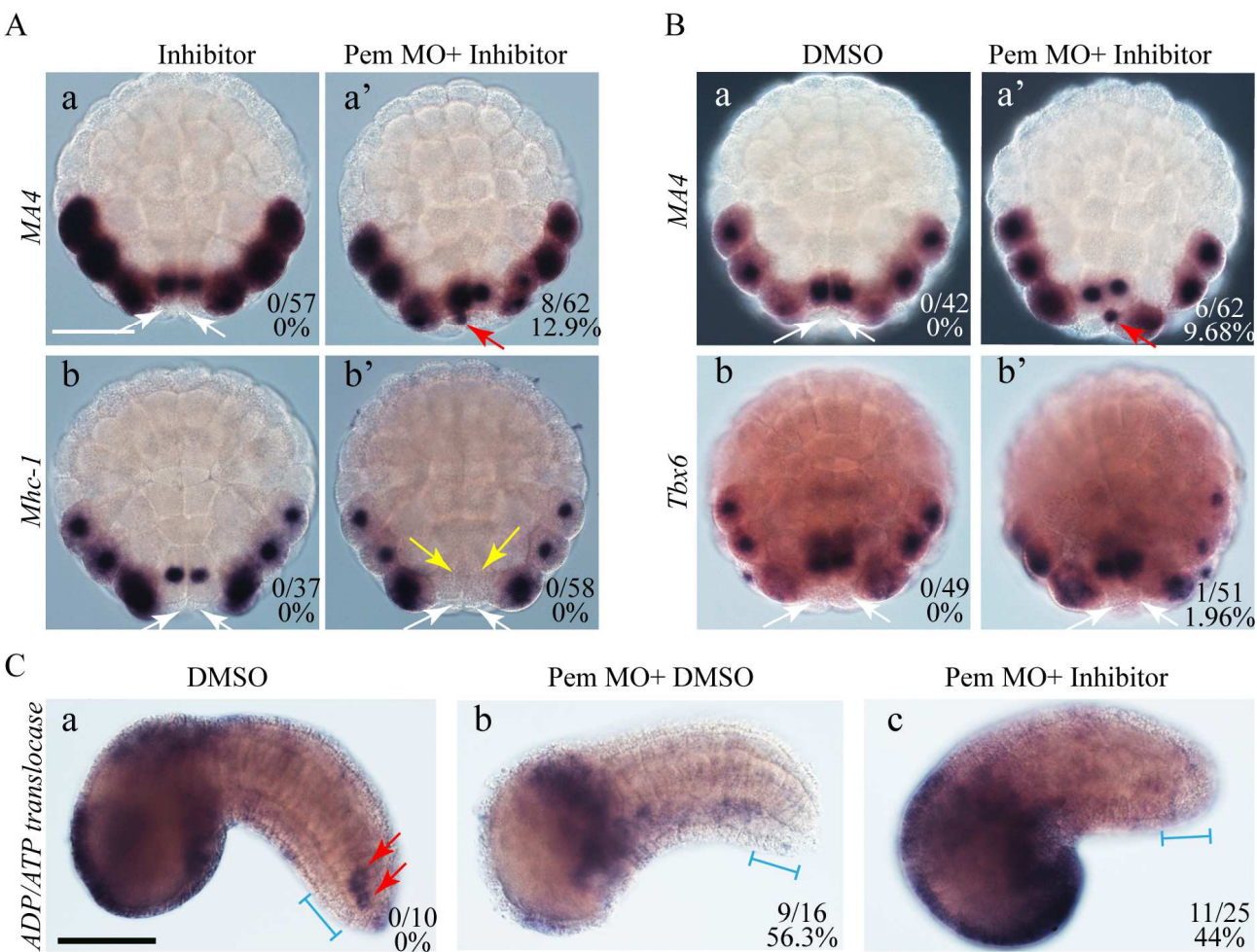
985
986

Fig. 6. Germline cells lacking Pem and H3K27me3 do not become fully differentiated muscle nor PGCs. Detection of *MA4* (A, B), *Mhc-I* (A) and *Tbx6* (B) expression at the 110-cell stage and of *ADP/ATP translocase* expression at the tailbud stage (C) by whole-mount *in situ* hybridization after different treatments (shown above images). Vegetal views with anterior up (A, B). Lateral views (C). White and red arrows in A and B indicate germline cells without or with ectopic gene expression, respectively. Yellow arrows indicate the loss of endogenous *Mhc-I* expression in B7.5. 74.1% of Pem- and H3K27me3-deficient embryos lost endogenous *Mhc-I* expression in B7.5 and 53.2% lost *MA4* expression. Red arrows in C indicate positive *ADP/ATP translocase* expression near the tip of the tail (light blue bars). Figures in the bottom right corner of each image show the relative number of embryos with ectopic gene expression (A, B) and without *ADP/ATP translocase* expression (C) in the germline. Scale bars, 100 µm.

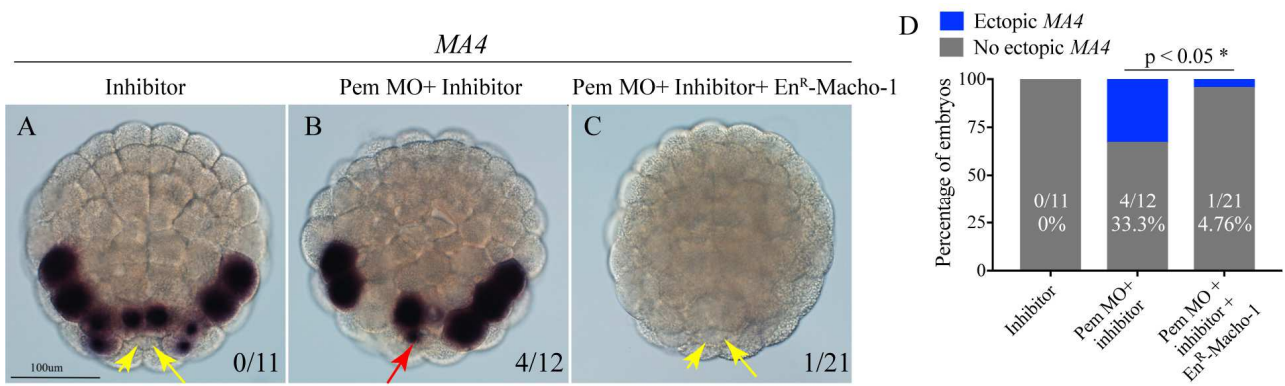
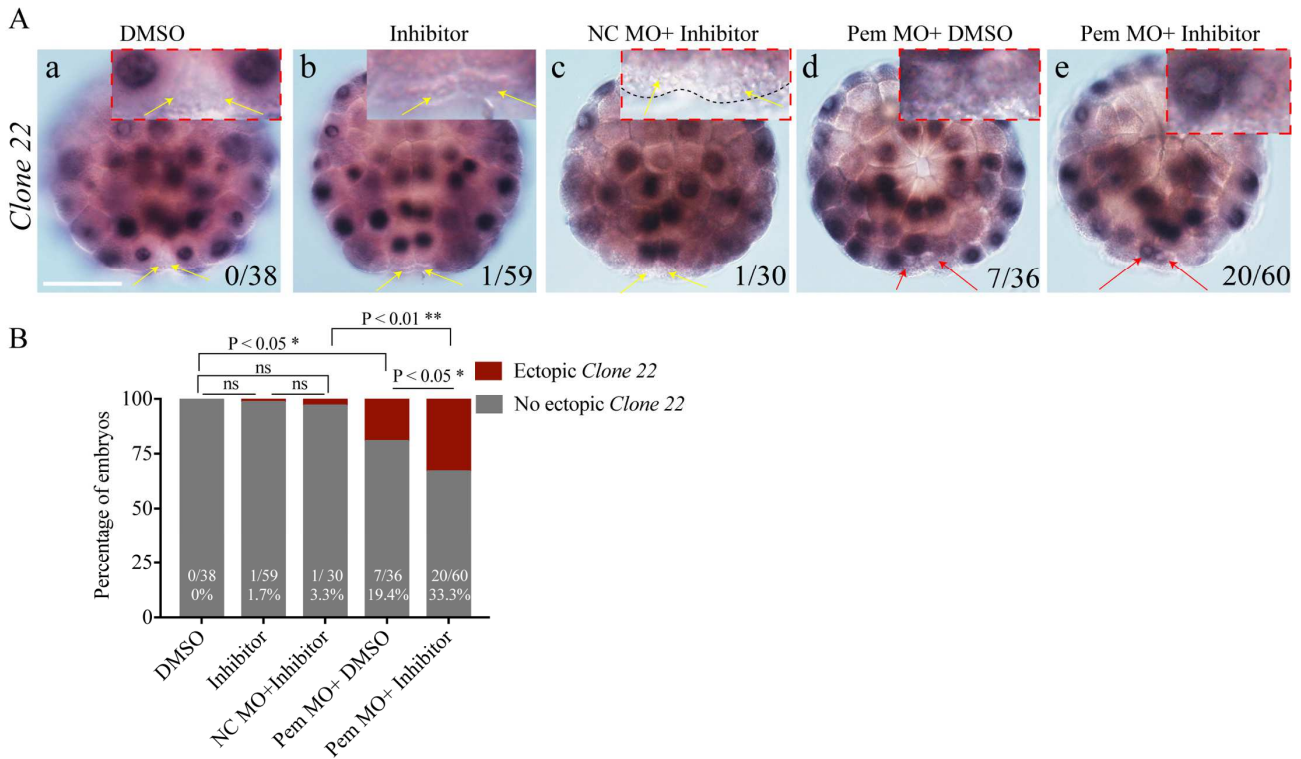
999
1000

Fig. 7. Inhibition of Macho-1 function eliminates mis-expression of *MA4* caused by Pem- and H3K27me3 downregulation. (A, B, C) Detection of *MA4* expression at the 110-cell stage by whole-mount *in situ* hybridization after different treatments (shown at the top of each image). Vegetal views with anterior up. Scale bar, 100 µm. Yellow and red arrows indicate the absence and presence, respectively, of ectopic *MA4* expression in the germline. Figures in the bottom right corner of each image are the relative number of embryos with ectopic *MA4* expression, illustrated in blue on a bar chart (D). The results of statistical analysis determined by two-tailed Fisher's Exact Test are shown above the bars.

1009

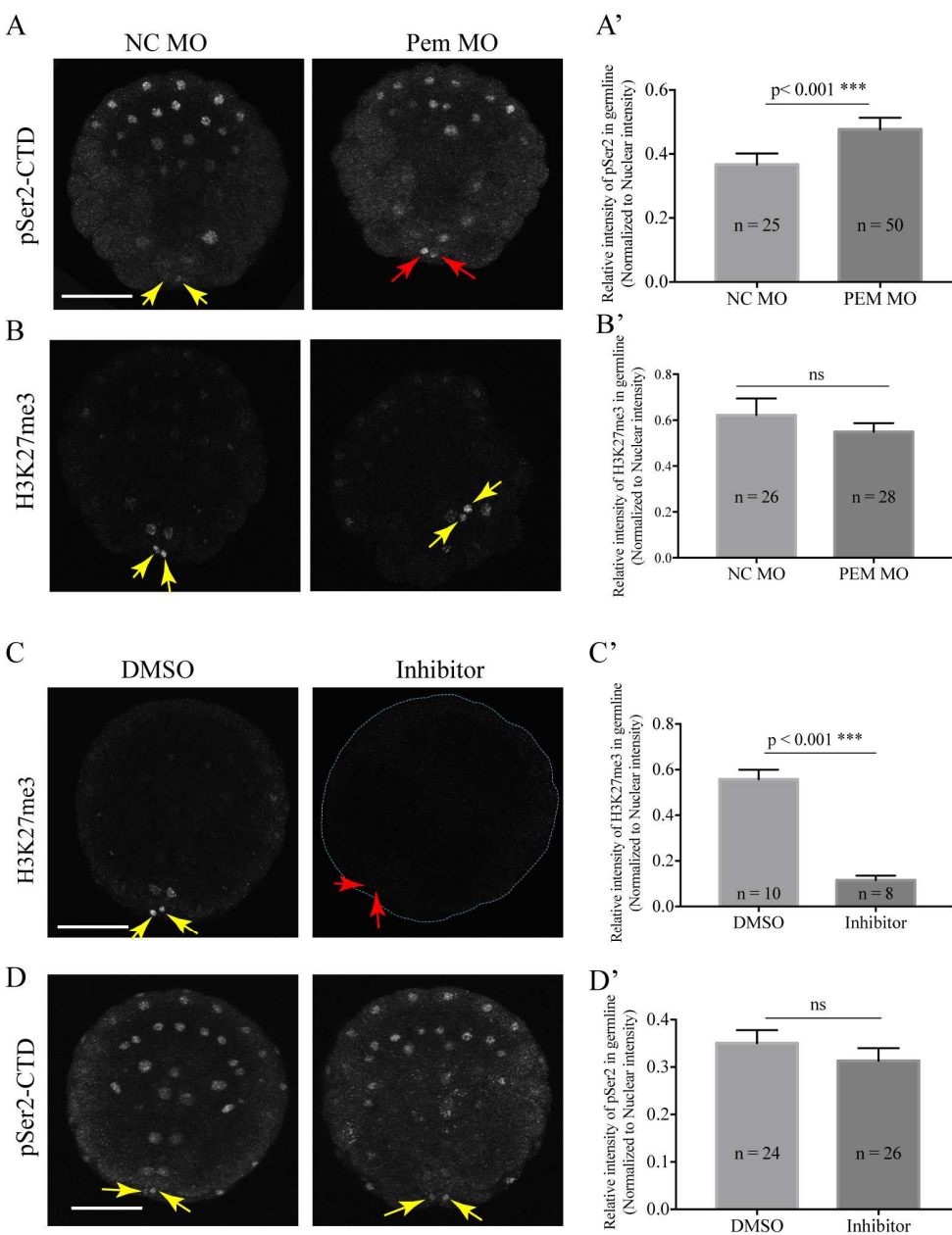


1010

1011

1012 Fig. 8. *Clone 22* is ectopically expressed in Pem-deficient, and Pem- and H3K27me3-deficient
 1013 germline cells. (A) Detection of *Clone 22* expression at the 110-cell stage by whole-mount *in situ*
 1014 hybridization after different treatments (shown above each image). Vegetal views with anterior up.
 1015 Scale bar, 100 μ m. Smaller insets in the top right corners are enlarged views of germline cells.
 1016 Yellow and red arrows indicate germline cells without or with ectopic *Clone 22* expression,
 1017 respectively. Figures in the bottom right corner of each image are the relative number of embryos
 1018 with ectopic *Clone 22* expression in germline cells, illustrated as a bar chart in (B) Percentage of
 1019 embryos with (red) or without (gray) expression in the germline. The results of statistical analysis
 1020 determined by two-tailed Fisher's Exact Test are shown above the bars (see Fig. S9 for further
 1021 details). ns, no significant difference.

1022

1023
1024

1025 Fig. 9. pSer2-CTD and H3K27me3 levels are regulated independently of each other. Vegetal
 1026 hemispheres of representative embryos with anterior up are shown in confocal Z-stack images.
 1027 Scale bars, 100 μ m. Immunostaining of 110-cell stage embryos with antibodies against pSer2-CTD
 1028 (A, D) and H3K27me3 (B, C). Embryos were injected with either NC MO or Pem MO (A, B), and
 1029 treated with DMSO or the inhibitor GSK126 (C, D). Red and yellow arrows indicate, respectively,
 1030 changed and unchanged immunostaining signal intensities in the germline cells when compared
 1031 with those in control embryos (NC MO injected and DMSO treated embryos). (A', B', C' and D')
 1032 Quantification of fluorescent signal intensities in the germline nuclei. The vertical scale indicates the

1033 intensities pSer2-CTD (A', D') or H3K27me3 (B', C') relative to those of SYTOX nuclear staining.

1034 The numbers of germline cells examined are shown on the bars. Statistical analysis was performed

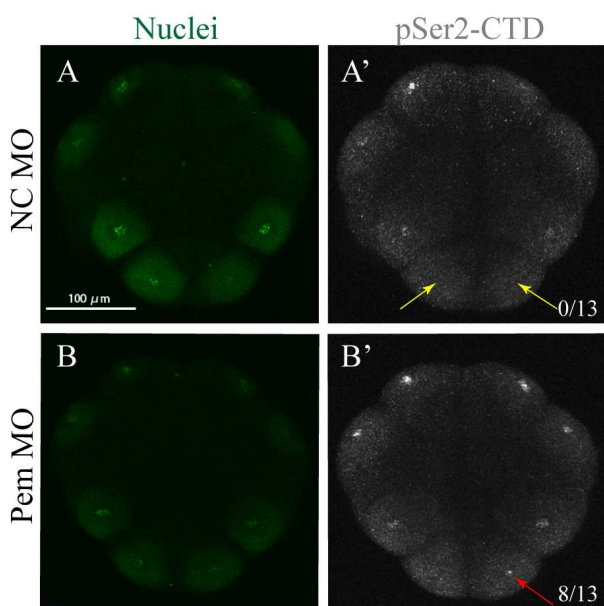
1035 using the Mann-Whitney U test. ns, no significant difference. Error bars indicate 95% confidence

1036 intervals.

1037

1038 Supplementary material

1039



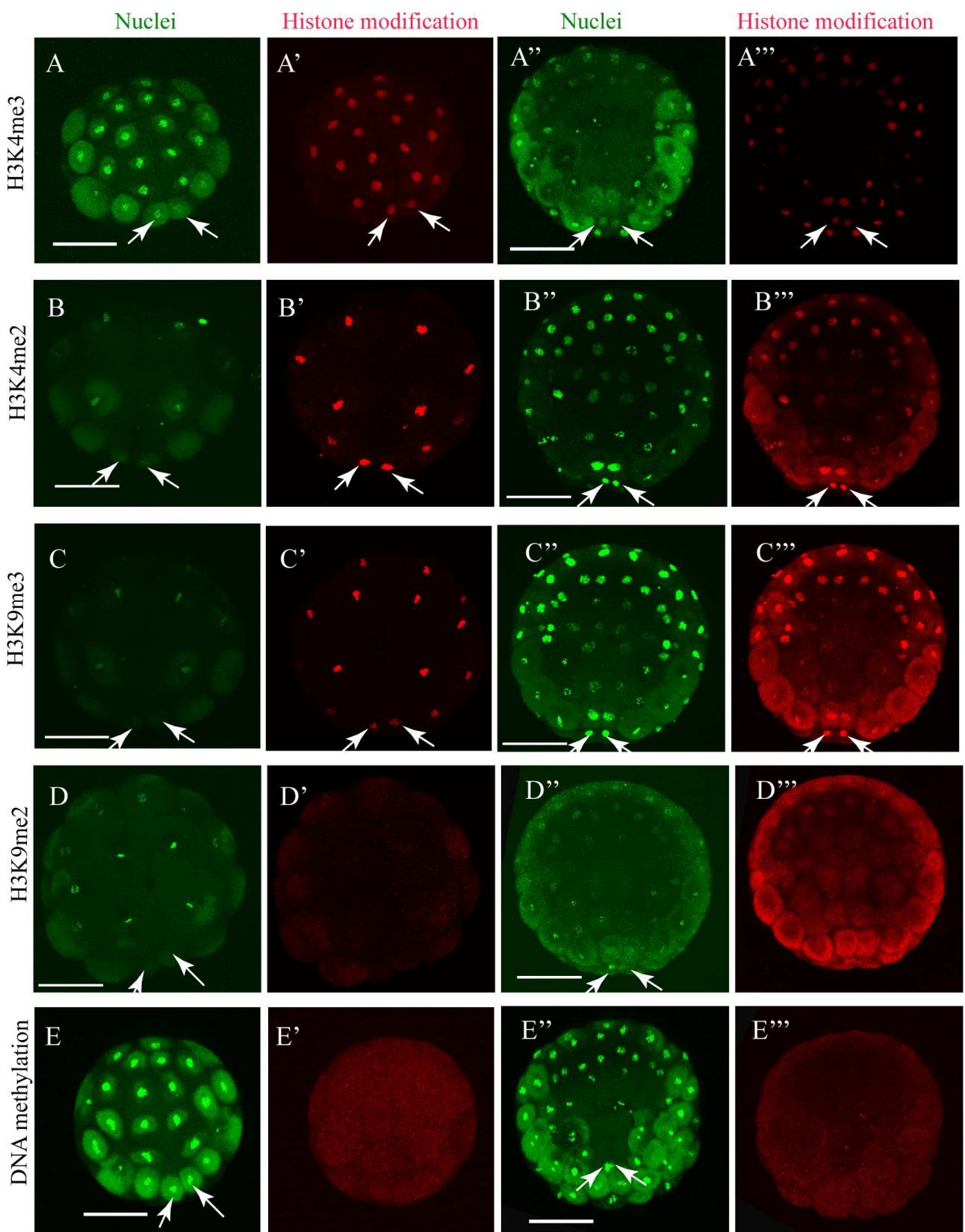
1040

1041

1042 Fig. S1. Pem MO injection de-represses the pSer2-CTD of RNAPII in the 16-cell stage germline
1043 cells. Vegetal hemispheres of representative embryos are shown with anterior up in the confocal
1044 Z-stack maximum projection. Scale bar, 100 μ m. (A, B) All nuclei were stained with SYTOX dye.
1045 (A', B') Immunostaining of the 16-cell stage embryos with an antibody against pSer2-CTD of
1046 RNAPII. Figures in the lower right corner are the relative number of embryos showing positive for
1047 germline pSer2-CTD of RNAPII. Yellow arrows and red arrows indicate, respectively, the negative
1048 and positive pSer2-CTD signals in the germline.

32-cell stage

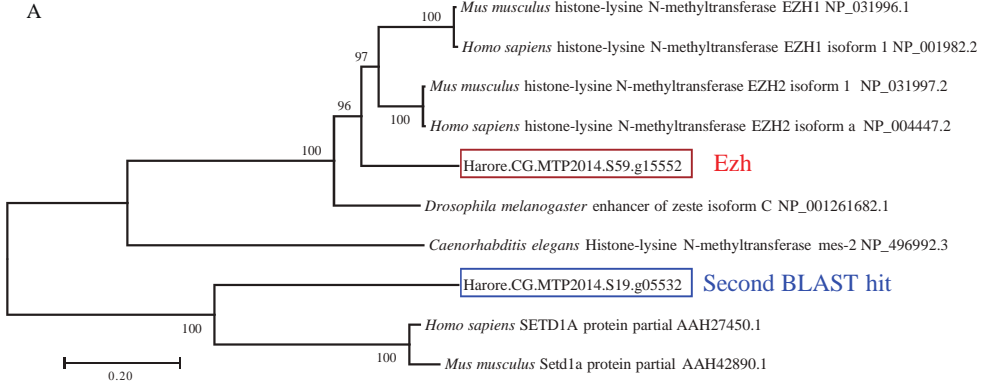
110-cell stage



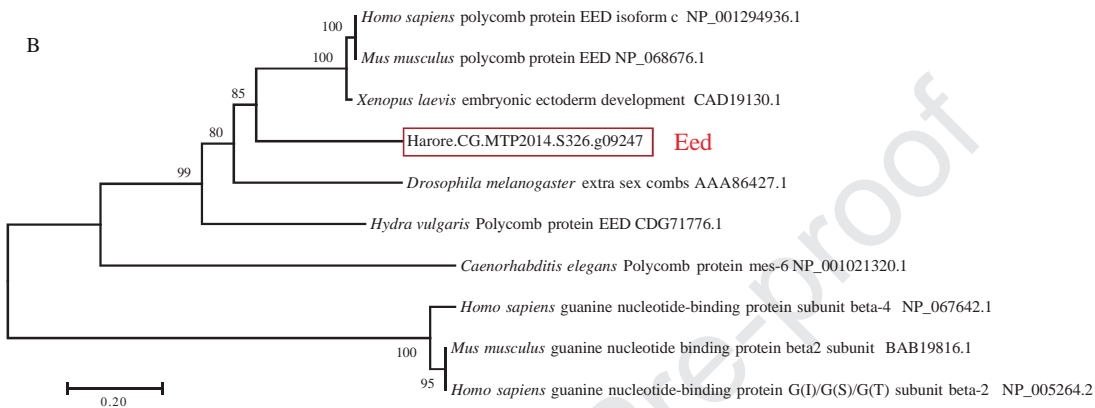
1054 Immunostaining of the 32- (A'-E') and 110-cell (A''-E'') stage embryos with antibodies against
1055 H3K4me3 (A', A''), H3K4me2 (B', B''), H3K9me3 (C', C''), H3K9me2 (D', D'') and DNA
1056 methylation (E', E''). Nuclei were stained with SYTOX green (A, A'', B, B'', C, C'', D, D'', E, E'').
1057 White arrows indicate the positions of the germline cells. Scale bars, 100 μ m.

1058

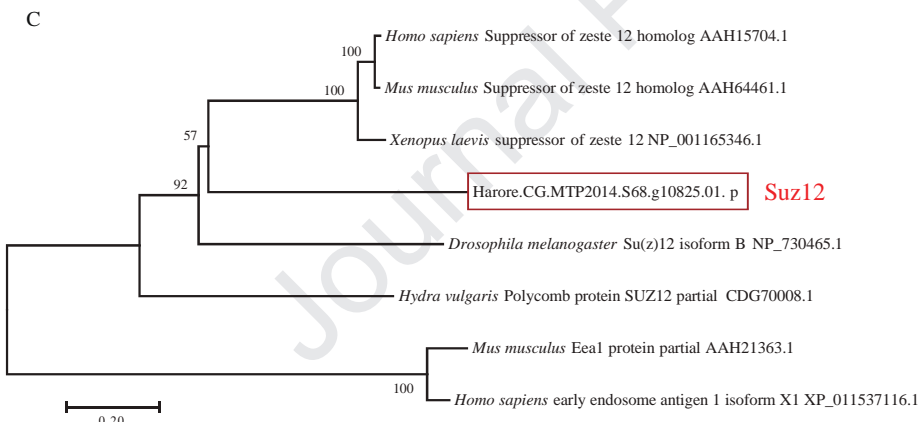
A



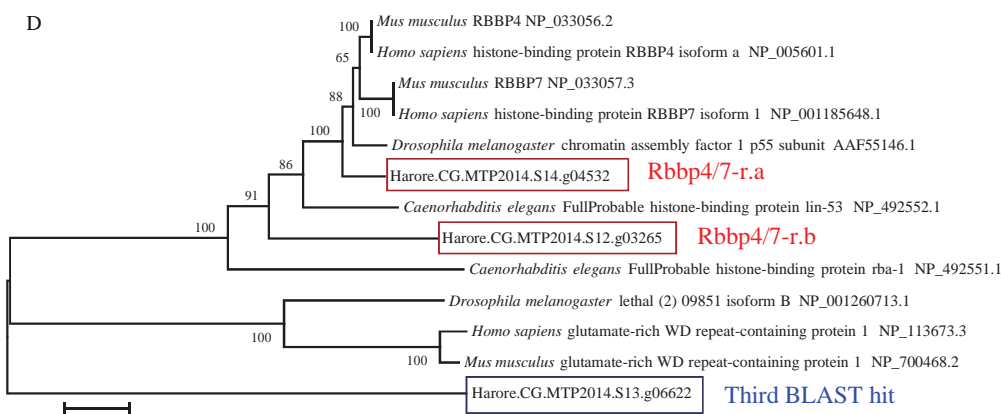
B



C



D



1059

1060 (Figure legend is on the next page.)

1061 Fig. S3. Phylogenetic trees for the core PRC2 components. Shown are *H. roretzi* orthologues
1062 (enclosed in red boxes) of EZH1/2 (A), EED (B), SUZ12 (C) and RBBP4/7 (D). The sequences
1063 enclosed in blue boxes are the second (B) or third (D) best hits resulting from BLAST searches.
1064 cDNA sequences of *Ezh*, *Eed*, *Suz12*, *Rbbp4/7-r.a* and *Rbbp4/7-r.b* in *H. roretzi* have been deposited
1065 in GenBank under accession numbers MN296499, MN296498, MN296496, MN296501 and
1066 MN296500, respectively.

1067

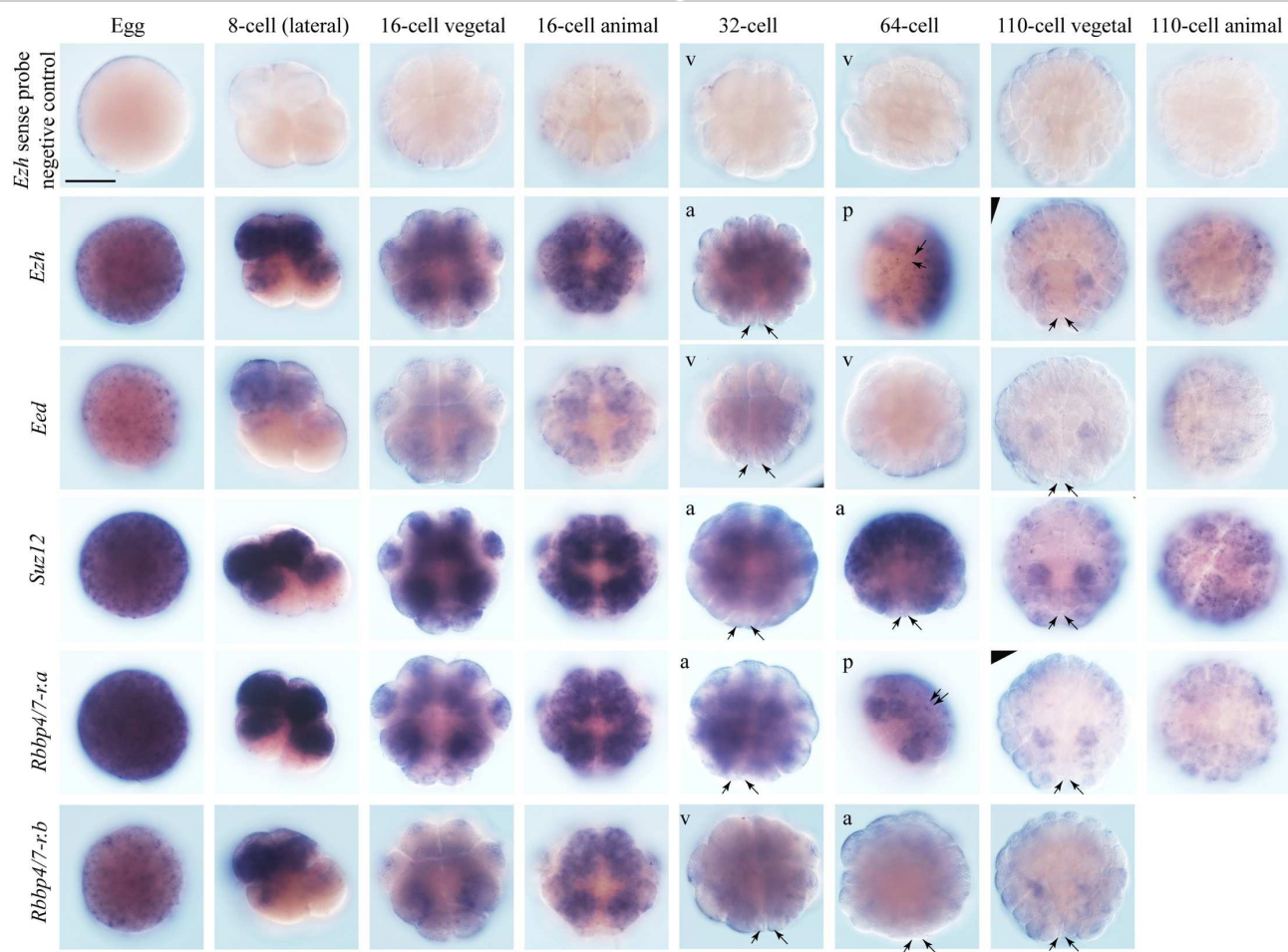
1068
1069

Fig. S4. All the core PRC2 components are maternally supplied with no enrichment in germline cells at later stages. Images of whole-mount *in situ* hybridization with DIG-labeled probes. Black arrows indicate germline cells without distinct signals. The positions of germline cells at the 64- and 110-cell stages were determined by nuclear staining (method as described in Fig. S7). Stages and aspects from which embryos are viewed are stated on the top with the exception of views for embryos at the 32- and 64-cell stages, which are shown in the upper left corner of each image: a, animal view; v, vegetal view; p, posterior view. Scale bar, 100 μ m.

1077

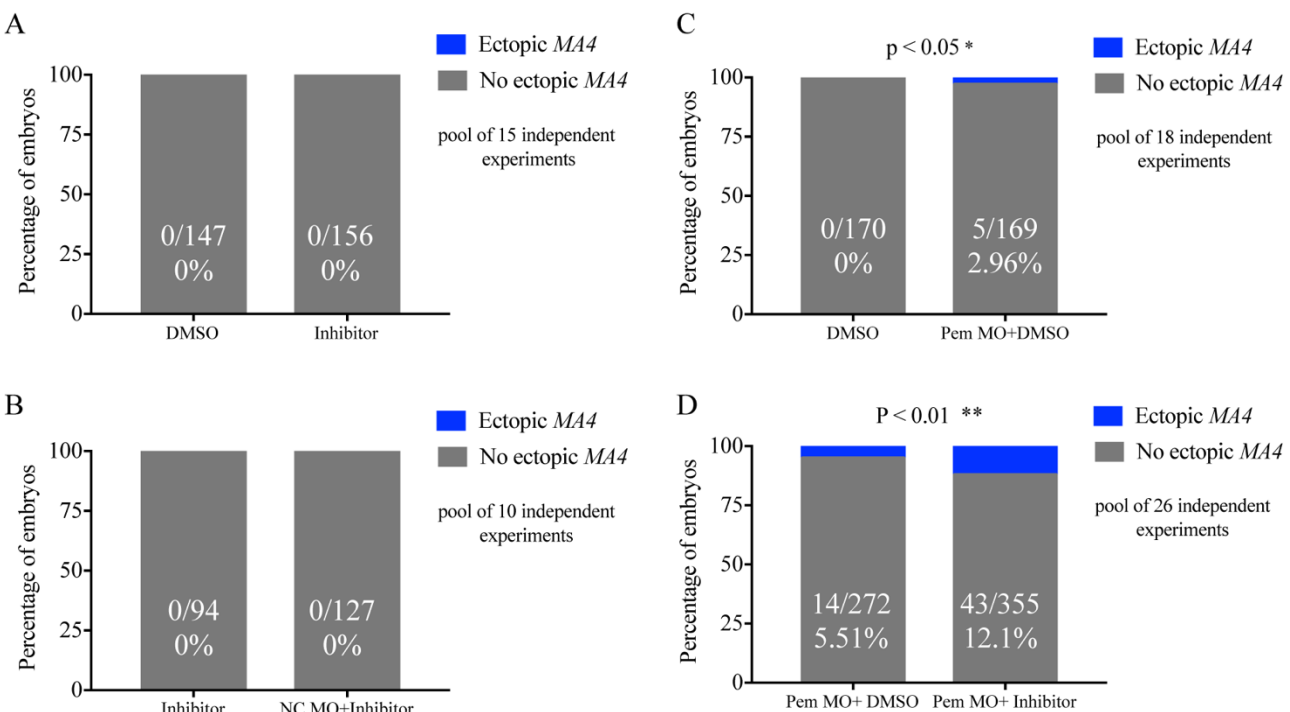
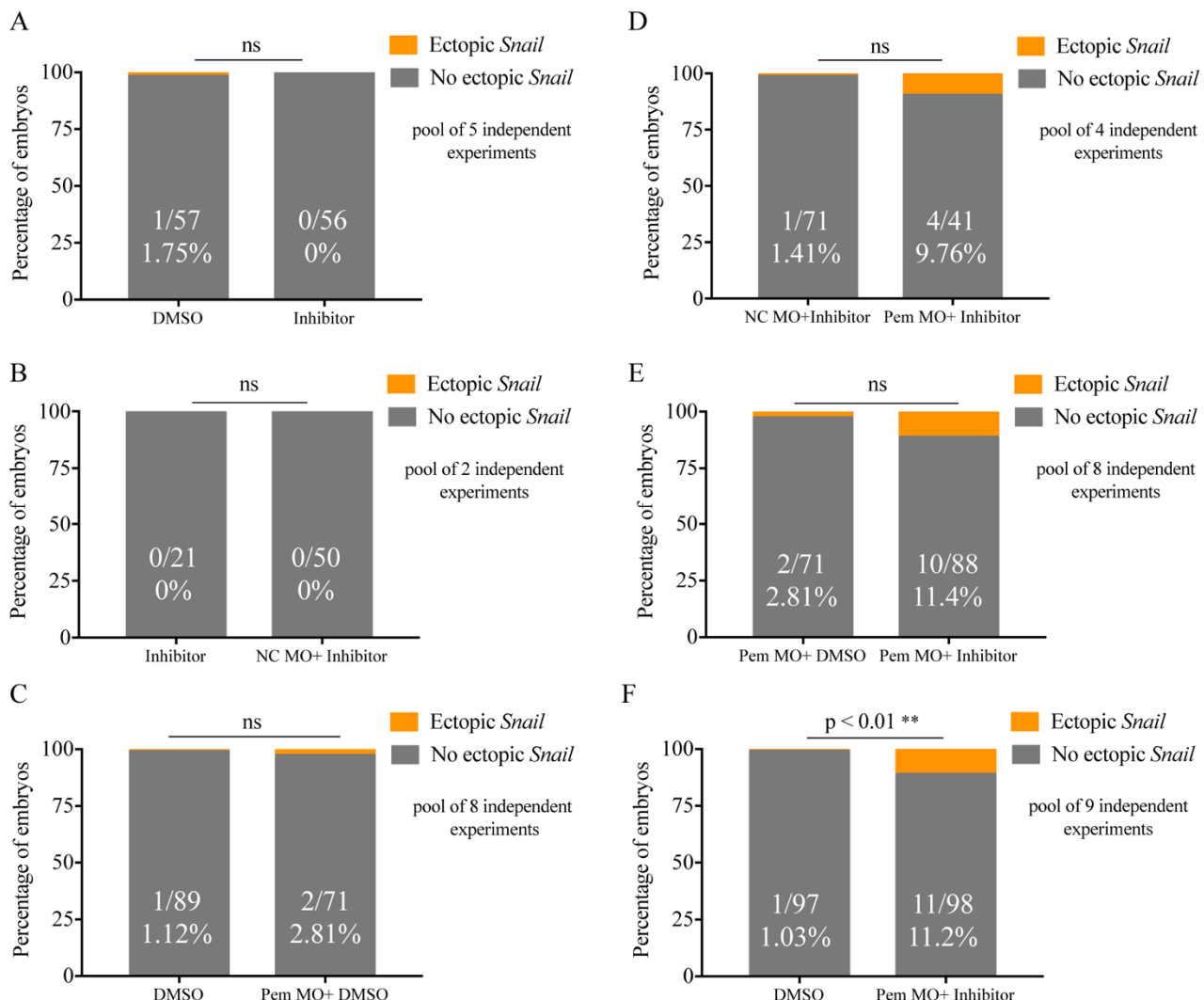
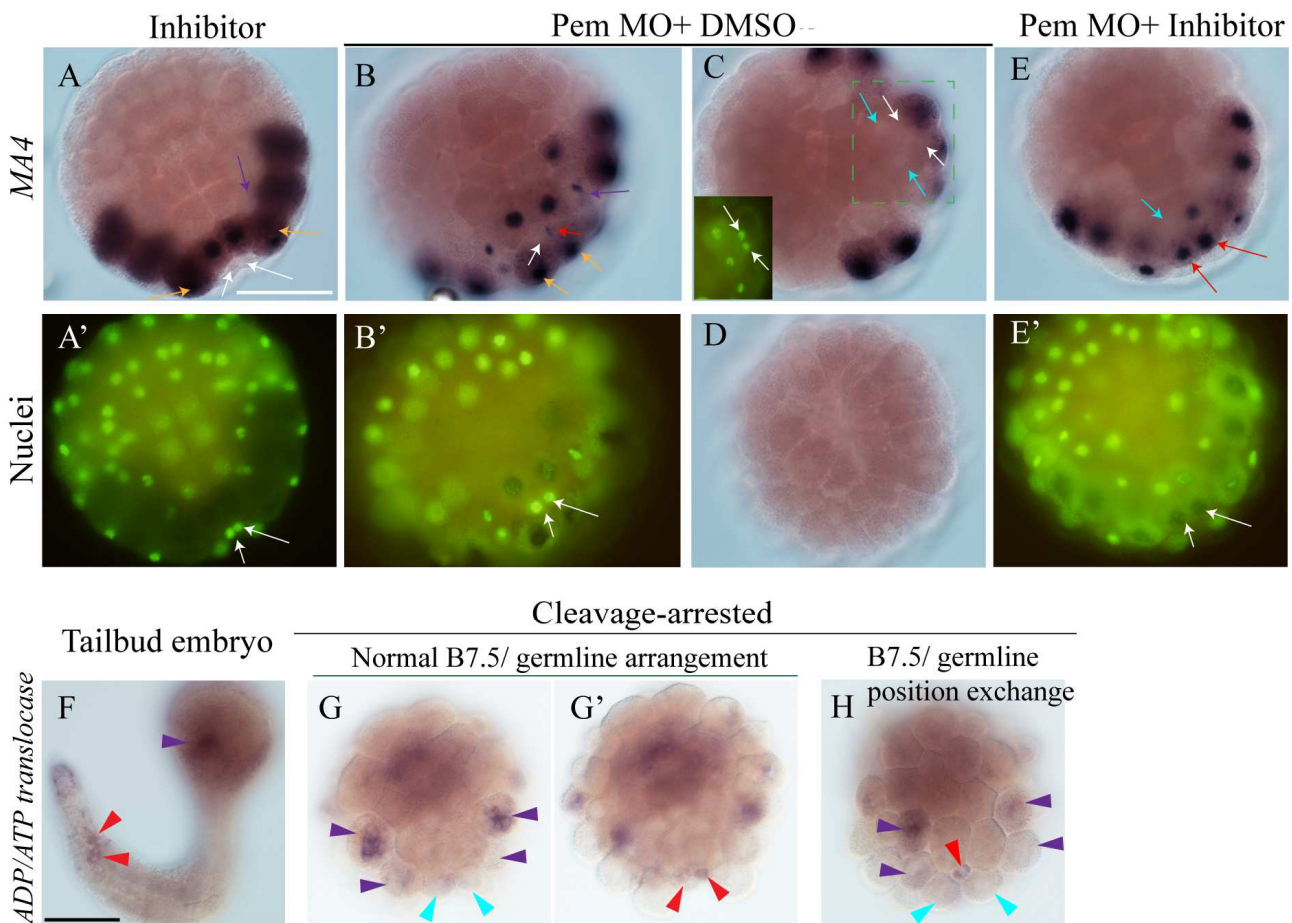
1078
1079

Fig. S5. Ectopic *MA4* gene expression appears in the germline of Pem-deficient, and Pem- and H3K27me3-deficient embryos. (A-D) The proportion of embryos showing ectopic *MA4* expression in the germline. The vertical scale indicates the percentage of embryos with or without ectopic *MA4* expression in the germline. The results of statistical analyses determined by two-tailed Fisher's Exact Test are shown above the bars. ns, no significant difference. For these statistical analyses, we set out to compare sets of two different treatment groups and select samples from the two groups only when they are from the same batch (originated from same fertilization). For example, in Fig. S5B (inhibitor vs NC MO + inhibitor), although the total number of inhibitor-treated and NC MO + inhibitor-treated embryos are 165 and 188, respectively (see Fig. 4C), the numbers of samples used for the statistical analysis are 94 for inhibitor and 127 for NC MO + inhibitor (Fig. S5B). In this case, for inhibitor and NC MO + inhibitor, respectively, 15 and 9 embryos from batch 1 were used, 7 and 12 from batch 2, 11 and 11 from batch 3, 6 and 15 from batch 4, 14 and 26 from batch 5, 9 and 12 from batch 6, 9 and 9 from batch 7, 7 and 10 from batch 8, 8 and 7 from batch 9, and 8 and 16 from batch 10.

1095
10961097 Fig. S6. Ectopic germline *Snail* expression appears in Pem- and H3K27me3-deficient embryos.

1098 (A-F) The proportion of embryos showing ectopic *Snail* expression in the germline. The vertical
 1099 scale indicates the percentage of embryos with (orange) or without (gray) ectopic *Snail* expression
 1100 in the germline. The results of statistical analyses determined by two-tailed Fisher's Exact Test are
 1101 shown above the bars. ns, no significant difference. Statistical analyses as Fig. S5.

1102



1103

1104

1105

1106

1107

1108

1109

1110

1111

1112

1113

1114

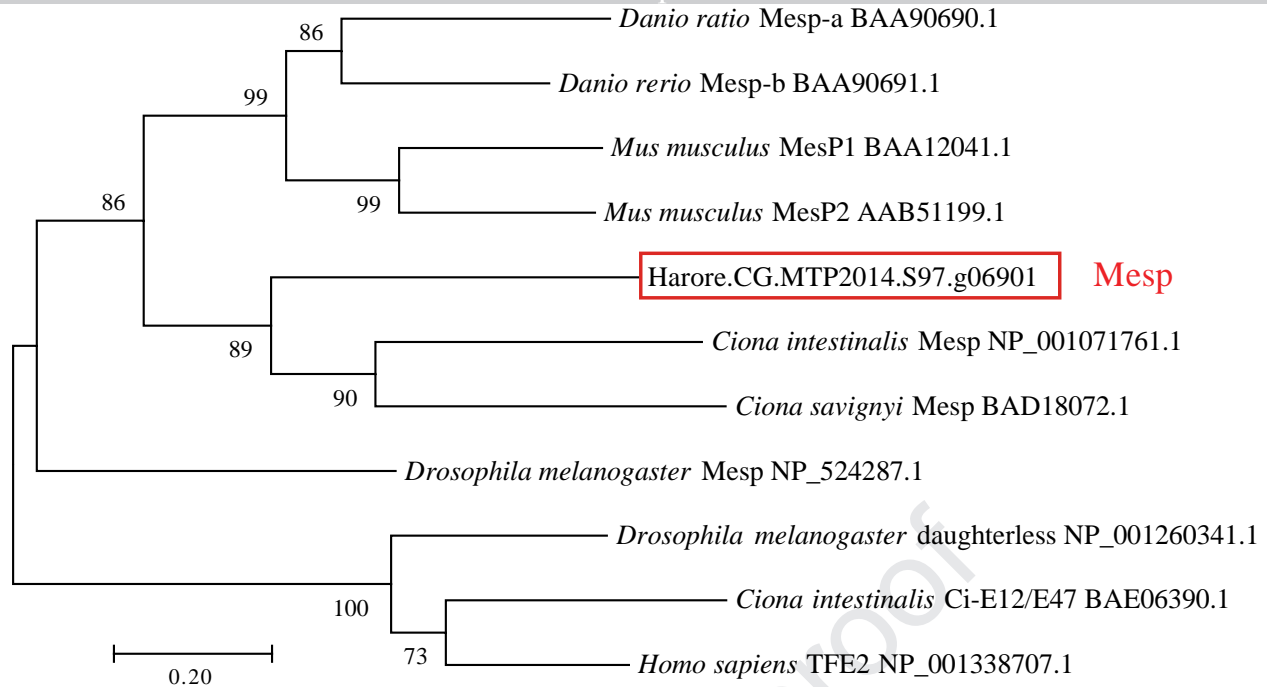
1115

1116

1117

Fig. S7. Examples of embryos showing abnormal cell cleavage pattern and loss of endogenous *MA4* expression. (A-E) Detection of *MA4* expression by whole-mount *in situ* hybridization after different treatments. Nuclei were stained with SYTOX (A', B', E' and inset in C). All vegetal views. Red and white arrows in A, B, C and E indicate ectopic and the absence of *MA4* expression, respectively, in germline cells; white arrows in A', B', E' and inset in C the positions of germline cells identified by nuclear staining and their smallest cell size; yellow arrows in A and B muscle-lineage B8.15 cells; purple arrows mesenchyme-lineage cells B7.7; light blue arrows in C and E the loss of endogenous *MA4* expression in B7.5 cells. Scale bar, 100 μ m. Normally (A), B7.7 mesenchyme cells (purple arrows) are located vegetally to the B8.15 muscle cells (yellow arrows). However, after Pem knockdown (B), the mesenchyme cells sometimes stuck out and pushed the B8.15 cells toward the midline of the embryo (yellow arrows); consequently, germline cells were no longer the posterior-most cells. (F-H, G') Detection of *ADP/ATP translocase* expression by whole-mount *in situ* hybridization in a control mid-tailbud embryo (F) and its equivalent stage embryos in which

1118 cell divisions were arrested from the 110-cell stage onwards by the treatment of Cytochalasin B (G,
1119 G', H). Lateral view (F). Vegetal views with anterior up (G, G', H). The image G' was captured in a
1120 deeper focal plane than G to show the germline cells in focus (red arrowheads in G') located behind
1121 the other vegetal cells shown in G (e.g. B7.5 cells, light blue arrowheads). Red arrowheads in F, G'
1122 and H indicate *ADP/ATP translocase* staining in germline cells; light blue arrowheads in G and H
1123 B7.5 cells; purple arrowheads in F, G and H mesenchyme-lineage cells. In some embryos from a
1124 late spawning season, germline cells swapped positions with their sister B7.5 cells even without
1125 Pem MO injection (H). In extreme cases where the cleavage pattern was disrupted completely,
1126 germline cells could not be identified. In such cases, when muscle signals were completely lost at
1127 the same time, as with the embryo in D, it was counted as “no ectopic”; but when signals were
1128 partially detected, it was not counted in any category.

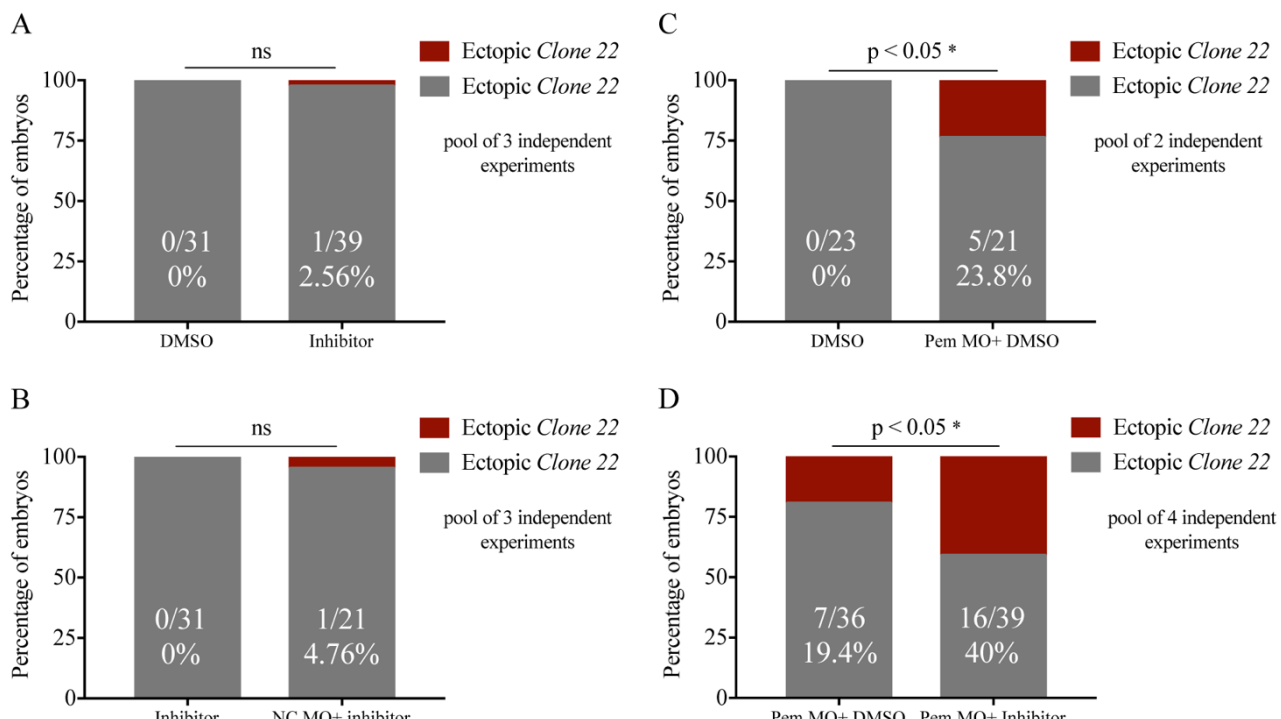


1129

1130

1131 Fig. S8. Orthologue of the *Mesp* gene in *H. roretzi*. A molecular phylogenetic tree constructed by
 1132 the neighbor-joining method based on alignment of the full-length amino acid sequences of *Mesp*
 1133 genes from different organisms and a putative *H. roretzi* *Mesp* gene (enclosed by the red box) found
 1134 by BLAST search. The number at each node is the bootstrap value (1000 replications). bHLH
 1135 domain-containing E-box proteins from different organisms were used as outgroups. The *Mesp* gene
 1136 in *H. roretzi* has been deposited in GenBank under accession number MN296497.

1137



1138

1139

1140 Fig. S9. Ectopic *Clone 22* gene expression appears in the germline of Pem-deficient, and Pem- and
 1141 H3K27me3-deficient embryos. (A-D) The proportion of embryos showing ectopic *Clone 22*
 1142 expression in the germline. The vertical scales indicate the percentage of embryos with or without
 1143 ectopic *Clone 22* expression in the germline. The results of statistical analysis determined by
 1144 two-tailed Fisher's Exact Test are shown above the bars. ns, no significant difference. Statistical
 1145 analyses were performed as Fig. S5.

1146
1147

		Early 16-cell	32-cell	64/110-cell
H3K4me2/3	Soma	+/-	+++	+++
	Germline	+/-	+++	+++
H3K9me3	Soma	++	+++	+++
	Germline	++	+++	+++
H3K9me2	Soma	-	-	-
	Germline	-	-	-
DNA methylation	Soma	-	-	-
	Germline	-	-	-
H3K27me3	Soma	-	+/-	+/-
	Germline	-	+/-	++

1148
 1149 Table S1. Summary of immunostaining against histone modifications and DNA methylation.
 1150 Symbol key: -, signal absent or almost undetectable; +/-, barely detectable; ++, clearly observed;
 1151 +++, detected strongly.

- 1 Highlights
- 2 H3K27me3 becomes enriched in ascidian germline cells from the 64-cell stage onwards.
- 3 Maternal germline silencer Pem suppresses RNAPII activity through the 110-cell stage.
- 4 H3K27me3- and Pem-deficient germline mis-expresses its sister muscle-lineage genes.
- 5 The mis-expression of muscle genes depends on a maternal determinant, Macho-1.